npj | biofilms and microbiomes

Article

Published in partnership with Nanyang Technological University

https://doi.org/10.1038/s41522-024-00546-0

Klebsiella pneumoniae AI-2 transporters mediate interspecies interactions and composition in a three-species biofilm community

Muhammad Zulfadhly Bin Mohammad Muzaki [1,2] ✉, Sujatha Subramoni [1], Stephen Summers [1], Staffan Kjelleberg [1,2] & Scott A. Rice [1,3,4] ✉

Biofilms in nature often exist as communities. In this study, an experimental mixed-species community consisting of *Pseudomonas aeruginosa*, *Pseudomonas protegens* and *Klebsiella pneumoniae* was used to investigate how AI-2 transporters affect interspecies interactions and composition. The *K. pneumoniae lsrB/lsrD* deletion mutants had a 10–25-fold higher concentration of extracellular AI-2 compared to the wild-type. Although these deletion mutants produced monospecies biofilms of similar biomass, the substitution of these mutants for the parental strain significantly altered composition. Dual-species biofilm assays demonstrated that the changes in composition were due to the cumulative effect of pairwise interactions. It was further revealed that *K. pneumoniae* being present physically in the consortium was important in AI-2 mediating composition in the consortium, and that AI-2 transporters were crucial in achieving maximum biomass in the community. In conclusion, these findings demonstrate that AI-2 transporters mediate interspecies interactions and is important in maintaining the compositional equilibrium of the community.

Biofilms are aggregates of microorganisms consisting of bacteria, yeast or algae, that adhere together and encase themselves within a matrix layer of Extracellular Polymeric Substances (EPS)[1]. These aggregates can either attach to a substratum (surface-attached biofilms), or to other cells, in suspended aggregates called flocs. Biofilms play a major role, both negatively and positively, in various industries such as in the marine and wastewater industries. Biofilms are a major challenge particularly in the health industry, where biofilms facilitate the progression of acute infections to chronic infections. For example, *P. aeruginosa* infection in Cystic Fibrosis (CF) patients are commonly associated with a co-infection with other pathogenic species, such as *Staphylococcus aureus*[2] and *Klebsiella pneumoniae*[3]. Therefore, interspecies interactions between co-pathogens play a crucial role in tackling biofilm-derived chronic infections. For example, previous reports showed that *Pseudomonas aeruginosa* and *Burkholderia cepacia*, which co-occur in some lung infections, exhibited unidirectional AHL-mediated communication, where AHLs produced by *P. aeruginosa* can be sensed by *B. cepacia*, but not vice versa. This unidirectional sensing of AHL signals enabled *B. cepacia* to improve its coordination of biofilm formation and virulence[4]. Hence, there is a growing appreciation for the prevalence of mixed-species biofilms and their involvement in various diseases, infections and wounds. This highlights the need for more studies elucidating the interactions and dynamics within these mixed-species biofilm communities. Understanding the interactions within species-specific contexts are important to successfully prevent or treat chronic infections involving mixed-species biofilms[5].

Competition and cooperation between members of the community are major drivers for shaping the spatial organization, composition and resilience of the mixed-species biofilm[6]. For example, *Burkholderia sp.* and *Pseudomonas sp.* formed separate, distinct microcolonies when grown in the presence of citrate, which they both can metabolize, displaying resource competition. When grown on chlorobiphenyl, which only *Burkholderia sp.* can metabolize, the two species co-aggregated strongly, suggesting a mutual or commensal sharing of metabolites[7]. It was determined that *Burkholderia sp.* releases the by-product chlorobenzoate during the metabolism of

[1]Singapore Centre for Environmental Life Sciences Engineering, Nanyang Technological University, Singapore, Singapore. [2]School of Biological Sciences, Nanyang Technological University, Singapore, Singapore. [3]The Australian Institute for Microbiology and Infection, The University of Technology Sydney, Sydney, NSW, Australia. [4]Microbiomes for One Systems Health and Agriculture and Food, CSIRO, Westmead, NSW, Australia. ✉e-mail: zulfadhlymuzaki@gmail.com; Scott.Rice@csiro.au

chlorobiphenyl, which was then utilized by *Pseudomonas sp.* as an energy source[7]. In a separate study, the presence of *Burkholderia sp.* within *P. aeruginosa* biofilms enhanced biofilm formation when compared to other species partners, which highlights the profound impact interspecies interactions can have on biofilm formation[8].

Therefore, to investigate the interspecies interactions within mixed-species biofilms and how these interactions shape the formation of the biofilm, an experimental three-species biofilm community was used as a model. This three-species biofilm community consists of *P. aeruginosa* PAO1, *Pseudomonas protegens* Pf-5 (renamed from *Pseudomonas fluorescens* Pf-5) and *K. pneumoniae* MGH78578. This three-species biofilm community has been shown to be highly reproducible in terms of biofilm structures and cell count[9–11]. In addition, this multispecies biofilm community is naturally occurring within soil, metalworking fluids[12] and the gut of a species of silk moth, *Bombyx mori*[13]. Furthermore, *K. pneumoniae* and *P. aeruginosa* are commonly isolated from the lungs of CF patients, which highlights their natural propensity to co-exist[3]. The clinical *K. pneumoniae* strain MGH78578 was chosen for this study due it being genetically tractable and the ease of making deletions in the strain. It was demonstrated that this three-species biofilm community displayed delayed biofilm development and exhibited distinct structures compared to single-species biofilm[11]. *K. pneumoniae* consistently dominated the biofilm after 72 h of growth, constituting approximately 80% of the community by volume. In addition, the same multispecies biofilm exhibited a community-level resistance to both Sodium Dodecyl Sulfate (SDS) and the antibiotic tobramycin. Additionally, the exopolysaccharides Pel and alginate were important in the establishment of *P. aeruginosa* within the mixed-species biofilm community[14]. Recently, we have further elucidated the role of acyl-homoserine lactone quorum sensing (AHL QS) in *P. aeruginosa* within the three-species community[15]. It was found that AHL QS in *P. aeruginosa* mediated the composition of the three-species community through competitive interactions between *P. aeruginosa* and *P. protegens*. Furthermore, it was established that these competitive interactions were mediated by the cumulative effects of AHL QS-regulated genes such as *rhlA*, *pqsA* and *pvdR*[15]. These findings show that although *P. aeruginosa* occupies only a small minority of the biomass in the community (1–5%), it plays a major role in establishing a stable composition within the mixed-species biofilm community along with *P. protegens* and *K. pneumoniae*, indicating that it functions as a keystone species within the community[15]. Furthermore, this study revealed that this three-species model community is useful in studying the effect of genes and signals in mediating interspecies interactions and community composition, owing to the consistent and reproducible proportions reached by three members of the community after 3 days of growth in continuous-culture conditions[15].

In this study, the role of QS in *K. pneumoniae* in mediating interspecies interactions and composition within the three-species biofilm community was investigated. With *K. pneumoniae* dominating the biomass of the three-species biofilm community (80–90%), it is expected to play a major role in influencing the ecological dynamics of the community. Instead of the AHL QS found in *P. aeruginosa*, the QS system present in *K. pneumoniae* is the autoinducer-2 quorum sensing (AI-2 QS) system. The signal for this QS system, autoinducer-2 (AI-2) is synthesized by the *luxS* gene, which is also is part of the activated methyl cycle (AMC), a metabolic pathway that is important for recycling of methyl groups[16,17]. AI-2 QS has been shown to mediate a variety of cellular processes, including bioluminescence[18], biofilm formation[19], capsule production[20], virulence[20], and motility[21]. *K. pneumoniae* possesses a bona fide AI-2 QS system, with *luxS* synthesizing the furanosyl borate diester AI-2 signal[22,23]. The regulatory network for AI-2 QS signaling in *K. pneumoniae* is dependent on the *lsrACDBFG* and *lsrRK* operons[24]. The *lsrACDB* genes code for a membrane-bound ATP-binding cassette transporter complex that functions to internalize the AI-2, which is then processed by LsrF and LsrG[24]. After processing, LsrK phosphorylates the AI-2 molecule and the AI-2-phosphate complex binds and inactivates the transcriptional repressor LsrR. LsrR represses the expression of the *lsrACDBFG* and *lsrRK* operons and therefore AI-2-phosphate regulates its own expression via a feedback loop[24].

LsrB is known to be a receptor for AI-2, which drives chemotaxis of the cell towards the signal, while LsrD is one of the proteins that make up the transmembrane channel proteins that facilitate the uptake of AI-2 signals back into the cell[25,26]. AI-2 has been shown to modulate the composition of mixed-species biofilms, for example, AI-2 production by *Streptococcus gordonii* mediates dual-species biofilm formation with *Porphyromonas gingivalis* through regulation of carbohydrate metabolism[27]. While the role of AI-2 QS (*luxS*) in *K. pneumoniae* monospecies biofilm formation has been studied[28,29], the effect of *K. pneumoniae* AI-2 on interspecies interactions within a mixed-species biofilm community is currently less well-known. Although chemically synthesized AI-2 has been shown to increase biofilm formation and virulence in *P. aeruginosa*[30,31], to date, there have been no studies investigating the role of the secretion and transport of AI-2 in mixed-species biofilms containing *K. pneumoniae*. In this study, the effect of deletion of the AI-2 receptor LsrB and the transmembrane AI-2 channel protein LsrD were investigated in mixed-species biofilms with *P. aeruginosa* PAO1 and *P. protegens* Pf-5. The loss of AI-2 sensing (LsrB) and AI-2 transport (LsrD) would be expected to result in increased extracellular AI-2 levels[32], which could impact neighboring species within the biofilm consortium via cross-talk. Previous studies have shown that a wide variety of bacterial species possess the ability to respond to the AI-2 signal, even without possessing the cognate LsrB or LuxP receptor, which led to the discovery of AI-2 as an "universal signal" for interspecies interactions[33,34]. Furthermore, as previously mentioned, we showed that AHL-based QS in *P. aeruginosa* influenced community composition by mediating interspecies interactions[15]. While *P. aeruginosa* occupied only 1–5% of biomass of the biofilm, *K. pneumoniae* dominates the biomass of the community biofilm (80–90%). Hence, it was of interest to study and compare the effects of different QS systems (AHL and AI-2 QS) in modulating community composition within two species of varying abundance (*P. aeruginosa* and *K. pneumoniae*) in the community. Therefore, in this study, the effect of AI-2 transporters *lsrB* and *lsrD* in *K. pneumoniae* MGH78578 were investigated in its ability to modulate monospecies biofilm formation, composition and interspecies interactions within the three-species biofilm community. This was achieved by deleting these genes in the clinically relevant strain *K. pneumoniae* MGH78578 and growing them as monospecies or multispecies biofilms in continuous-culture biofilms in the standard laboratory medium M9. Results showed that deletion of *lsrB* and *lsrD* resulted in higher extracellular AI-2 concentration, but no significant changes in biomass of single-species *K. pneumoniae* biofilms. However, substitution of the wild-type *K. pneumoniae* with the *lsrB*/*lsrD* mutants resulted in a major change in composition of the three-species biofilm community, due to changes in *lsrB*/*lsrD*-mediated interspecies interactions.

Results

Deletion of LsrB and LsrD AI-2 transporter proteins results in decreased AI-2 uptake in planktonic cultures of *K. pneumoniae* MGH78578

Whole-genome sequencing of *K. pneumoniae* MGH78578 Δ*lsrB* and Δ*lsrD* deletion mutants showed that there was a correct deletion in the genes of interest in all both mutant strains. Analysis of the genome sequences detected no INDELS present in any of the mutant strains, However, 1 SNP in the Δ*lsrB* mutant was detected, which resulted in a Tyr to Asn conversion in a putative alkaline phosphatase isozyme conversion protein.

An autoinducer-2 (AI-2) plate assay was performed on the planktonic supernatants of *K. pneumoniae* MGH78578 *lsrB* and *lsrD* mutants. Of the three species in the community, *K. pneumoniae* MGH78578 secreted significantly higher levels of extracellular AI-2 (22.4 ± 3.0 RLU), compared to *P. aeruginosa* (2.4 ± 2.3 RLU) and *P. protegens* (3.7 ± 3.2 RLU), and therefore is the main contributor of extracellular AI-2 in the community (Fig. 1a). The addition of pUCP22 plasmid did not result in any significant changes in level of extracellular AI-2 (Fig. 1a). Comparison of RLU showed that deletion of the *lsrB* and *lsrD* genes in planktonic cultures resulted in a

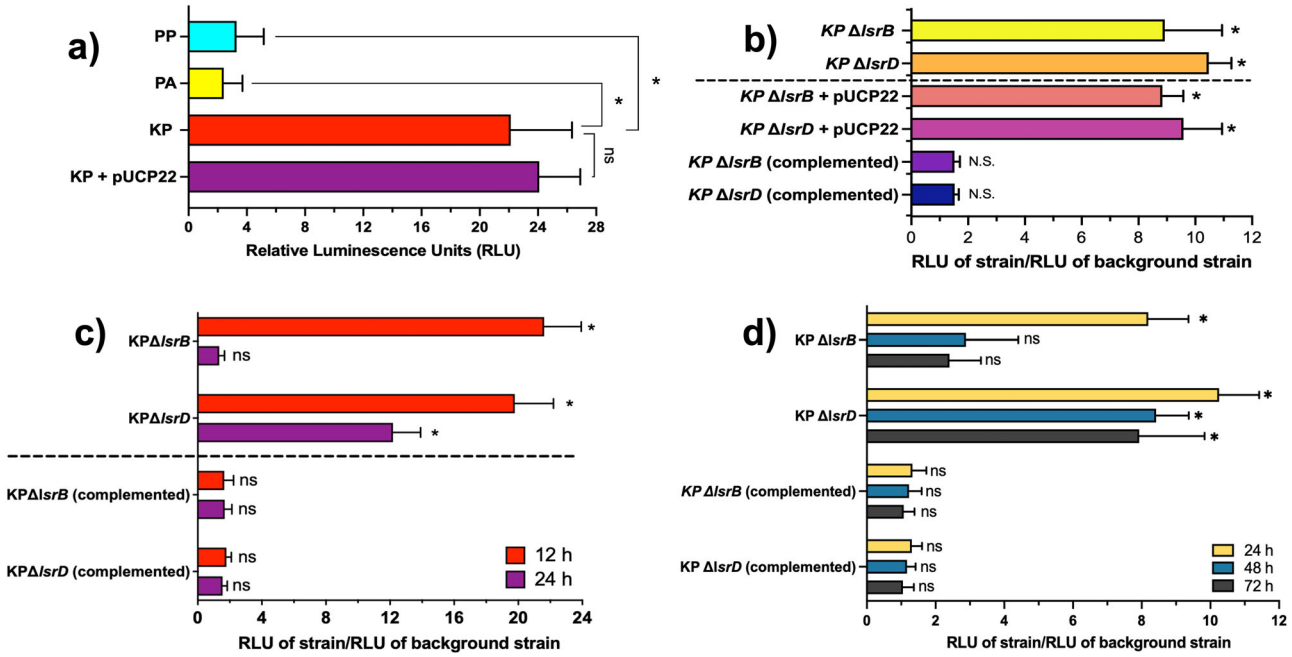

Fig. 1 | AI-2 bioassay to measure the relative level of AI-2 in cell-free supernatants. a Peak relative luminescence units (RLU) of the planktonic supernatants of *K. pneumoniae* (KP), *K. pneumoniae* with pUCP22 plasmid (KP + pUCP22), *P. aeruginosa* (PP) and *P. protegens* (PP) strains. Peak RLU was achieved at $t = 180$ mins. $N = 3$ independent replicates, * represents a significant difference ($P < 0.001$), ns represents no significant difference. **b** Comparison of the level of AI-2 present in the cell-free supernatants (CFS) of planktonic cultures of *K. pneumoniae* Δ*lsrB* and Δ*lsrD* mutants with or without pUCP22) and complemented strains compared to their respective background strains (*K. pneumoniae* wild-type and *K. pneumoniae* wild-type + pUCP22, respectively) after 12 h of growth. Peak RLU of strains measured at $t = 180$ min. $N = 9$, three independent replicates. ns denotes no significant change, * represents a significant difference ($P < 0.001$). **c** Comparison of the level of AI-2 present in the CFS of planktonic cultures of *K. pneumoniae* Δ*lsrB* and Δ*lsrD* mutants and complemented strains compared to their respective background strains (*K. pneumoniae* wild-type and *K. pneumoniae* wild-type + pUCP22, respectively) after 12 and 24 h. Peak RLU of strains measured at $t = 180$ min. $N = 3$ independent replicates. ns denotes no significant change, * represents significant difference ($P < 0.001$). **d** Comparison of the level of AI-2 present in the cell-free flow-through of the continuous-culture biofilms of *K. pneumoniae* Δ*lsrB* and Δ*lsrD* mutants and complemented strains compared to their respective background strains (*K. pneumoniae* wild-type and *K. pneumoniae* wild-type + pUCP22, respectively) after 24, 48, and 72 h. Peak RLU of strains measured at $t = 180$ min. $N = 3$ independent replicates. ns denotes no significant change, * represents a significant difference ($P < 0.001$).

significant increase ($P < 0.001$) in peak RLU compared to the wild-type (8.9 ± 2.0-fold and 10.4 ± 0.8-fold, respectively) (Fig. 1b). The addition of pUCP22 did not result in significant changes in extracellular AI-2 levels compared to its wild-type background strain, while complementation of *lsrB* and *lsrD* in the respective mutants resulted in the restoration of the wild-type levels of AI-2 (Fig. 1b). This also suggests that the SNP in the Δ*lsrB* in the putative alkaline phosphatase enzyme was not responsible for the elevated levels of AI-2 in this mutant. Similarly, the relative level of extracellular AI-2 in the batch biofilm culture supernatant (Fig. 1c) was quantified for the *K. pneumoniae* MGH78578 strains. The level of extracellular AI-2 was significantly higher ($P < 0.001$) in the Δ*lsrB* (21.6 ± 5.2-fold) and Δ*lsrD* (19.8 ± 3.8-fold) mutants compared to the wild-type strain after 12 h of biofilm growth. Interestingly, while the level of AI-2 produced by *K. pneumoniae* Δ*lsrD* mutant remained significantly higher (12.2 ± 1.7-fold) than the wild-type after 24 h of biofilm growth, this was not the case for the Δ*lsrB* mutant, which not significantly different (1.3 ± 0.3-fold) to the wild-type after 24 h. This same trend was also observed in continuous-culture biofilms (Fig. 1d). These results demonstrate that the deletion of the *lsr* genes resulted in a significant increase (10–20-fold) in the concentration of extracellular AI-2 in planktonic and 12h-biofilm conditions, due to the loss of the ability of the *lsr* mutants to internalize AI-2.

Deletion of *lsrB* and *lsrD* in *K. pneumoniae* did not affect growth rate, monospecies biofilm formation, and autoaggregation in planktonic cultures

The planktonic growth rates, monospecies biofilm formation and autoaggregation phenotypes of *K. pneumoniae* wild-type, *lsrB* and *lsrD* deletion mutants were determined (Fig. 2). The growth curve (Fig. 2a) and growth rate (Fig. 2b) of *K. pneumoniae* Δ*lsrB* (0.43 ± 0.02/h) and Δ*lsrD* (0.42 ± 0.01/h) deletion mutants were not significantly different to their isogenic wild-type strain (0.44 ± 0.02/h). Furthermore, there was no significant difference in biofilm biomass of *K. pneumoniae* Δ*lsrB* ($OD_{600} = 0.44 \pm 0.06$ and $4.71 \pm 0.29\ \mu m^3/\mu m^2$, respectively) or the Δ*lsrD* ($OD_{600} = 0.45 \pm 0.08$ and $3.67 \pm 0.30\ \mu m^3/\mu m^2$, respectively) mutants compared to wild-type in batch biofilm cultures as well as continuous-culture biofilms (Fig. 2c, d), as determined by confocal microscopy (Fig. 2c, d) and crystal violet assay (Fig. 2e). In addition, deletion of *lsrB* and *lsrD* did not result in any differences in the autoaggregation in *K. pneumoniae* (Fig. 2f).

The loss of *lsrB* and *lsrD* in *K. pneumoniae* results in a significant change in mixed-species biofilm composition

To determine the role of AI-2 transporters within a mixed-species biofilm community, *K. pneumoniae* Δ*lsrB* and Δ*lsrD* mutants were grown in continuous-culture biofilms with *P. aeruginosa* and *P. protegens* for 3 days (Fig. 3a). While the deletion of *lsrB* or *lsrD* did not significantly change monospecies biofilm formation of *K. pneumoniae* (Fig. 2c–e), deletion of these genes resulted in a significant change in the mixed-species biofilm composition. Deletion of *lsrB* resulted in a significant decrease ($P < 0.05$) in the proportion of *K. pneumoniae* (74.5 ± 6.7% to 67.5 ± 10.9%) and in *P. aeruginosa* (6.2 ± 3.9% 1.2 ± 1.0%), as well as a significant increase in the proportion of *P. protegens* (19.2 ± 7.4% 31.3 ± 10.9%) (Fig. 3a, b). The changes in composition within the mixed-species biofilm community was associated with a significant decrease ($P < 0.05$) in the biovolume of *K. pneumoniae* (−38.3 ± 4.6%) and *P. aeruginosa* (−83.9 ± 3.5%) and a significant increase in the biovolume of *P. protegens* (+40.9 ± 12.4%) (Fig. 3c). Similarly, substitution of the

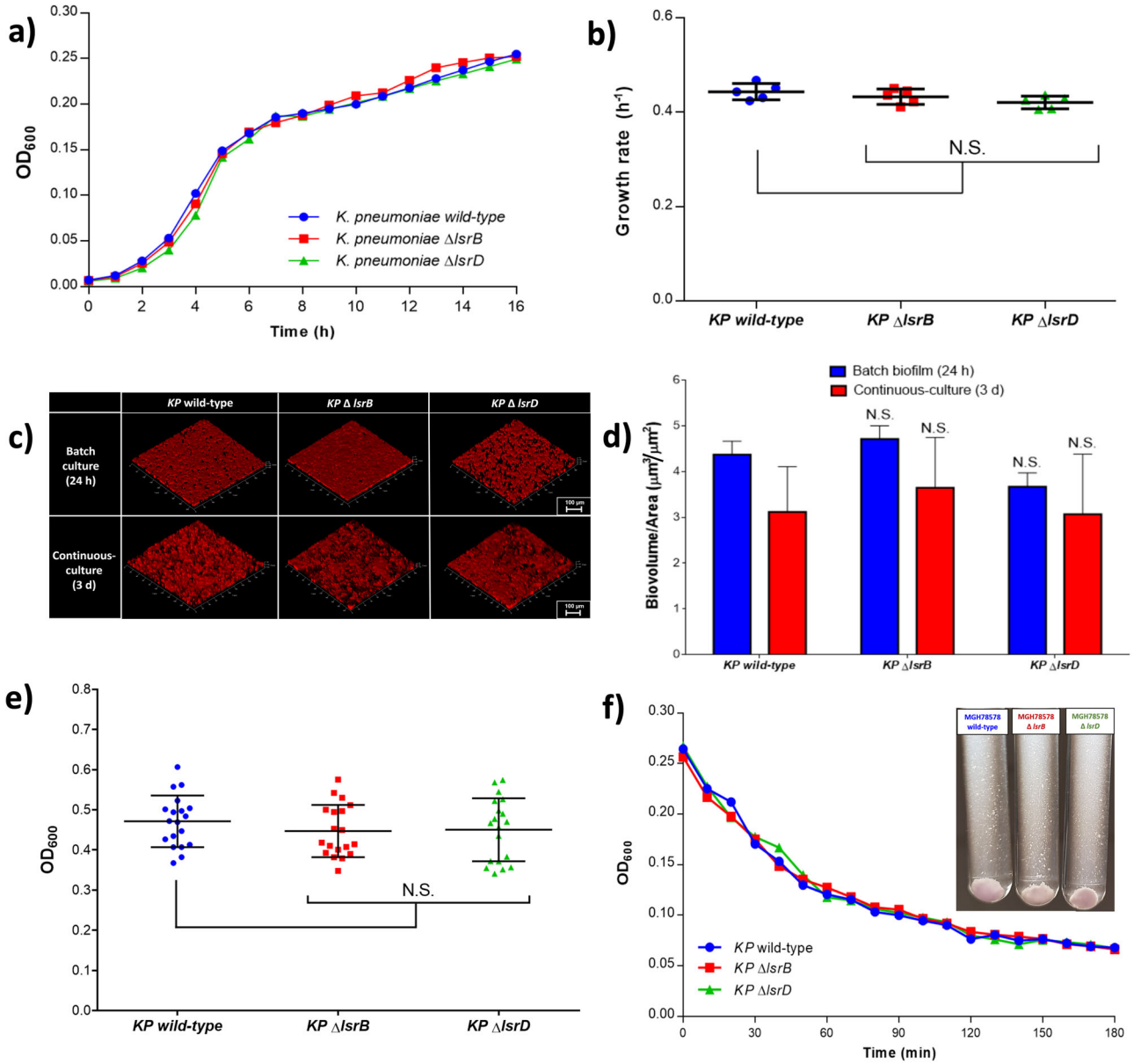

Fig. 2 | Phenotypes tested for *K. pneumoniae* Δ*lsrB* and Δ*lsrD* mutants. Comparison of **a** growth curves and **b** growth rates of *K. pneumoniae* strains grown in M9CasGlucose medium. Growth rates were calculated from the logarithmic growth phase from $t = 2$ h to $t = 6$ h. ($N = 5$ biological replicates, N.S. represents no significant change, error bars represent standard deviation). **c** Representative three-dimensional confocal laser scanning microscopy images and **d** biovolume/area of single-species biofilms formed by *K. pneumoniae* strains grown under batch conditions for 24 h within 24-well glass-bottomed plates and under continuous-culture conditions within flow chambers for 3 days. Scale bars represent 100 μm ($N = 6$ biological replicates, N.S. represents no significant change, and error bars represent standard deviation). **e** Crystal violet assay quantifying the biomass of single-species biofilms of *K. pneumoniae* strains grown in 24-well plates in M9CasGlucose for 24 h ($N = 20$ biological replicates, N.S. denotes no significant change, error bars represent standard deviation). **f** Settling assay and representative images of aggregates formed by *K. pneumoniae* strains after 180 min grown in M9CasGlucose medium ($N = 3$ biological replicates).

wild-type *K. pneumoniae* with the Δ*lsrD* mutant resulted in a significant decrease ($P < 0.05$) in the proportion of *K. pneumoniae* (74.5 ± 6.7% to 40.1 ± 12.3%) and *P. aeruginosa* (6.2 ± 3.9% to 2.1 ± 2.3%), as well as a significant increase in the proportion of *P. protegens* (19.2 ± 7.4% to 57.8 ± 11.9%) (Fig. 3b). Accordingly, the biovolumes of *K. pneumoniae* (−72.3 ± 12.0%) and *P. aeruginosa* (−93.6 ± 1.3%) were significantly lower ($P < 0.05$), while there was a significant increase ($P < 0.05$) in the biovolume of *P. protegens* (+ 54.7 ± 6.1%) (Fig. 3c). The addition of an empty pUCP22 plasmid vector into the *K. pneumoniae* Δ*lsrB* and Δ*lsrD* mutants still resulted in the same trends in the changes in community composition compared to the wild-type background strain (*K. pneumoniae* wild-type + pUCP22) (Fig. 3b). Similarly, complementation of the *lsrB* and *lsrD* mutants did not result in a significant change in relative abundances of the community members compared to when the background wild-type *K. pneumoniae* was present. When complemented strains of Δ*lsrB* and Δ*lsrD* were present instead of the wild-type background strain, the proportions of *K. pneumoniae* (77.2 ± 8.4% and 74.9 ± 11.6%, respectively), *P. aeruginosa* (5.5 ± 5.4% and 6.0 ± 3.1%, respectively) and *P. protegens* (17.2 ± 8.2% and 18.9 ± 9.3%, respectively) were not significantly altered (Fig. 3b). The addition of an empty pUCP22 plasmid vector into the *K. pneumoniae* Δ*lsrB* and Δ*lsrD* mutants still resulted in the same trends in the changes in community composition compared to the wild-type background strain (*K. pneumoniae* wild-type + pUCP22) (Fig. 3b).

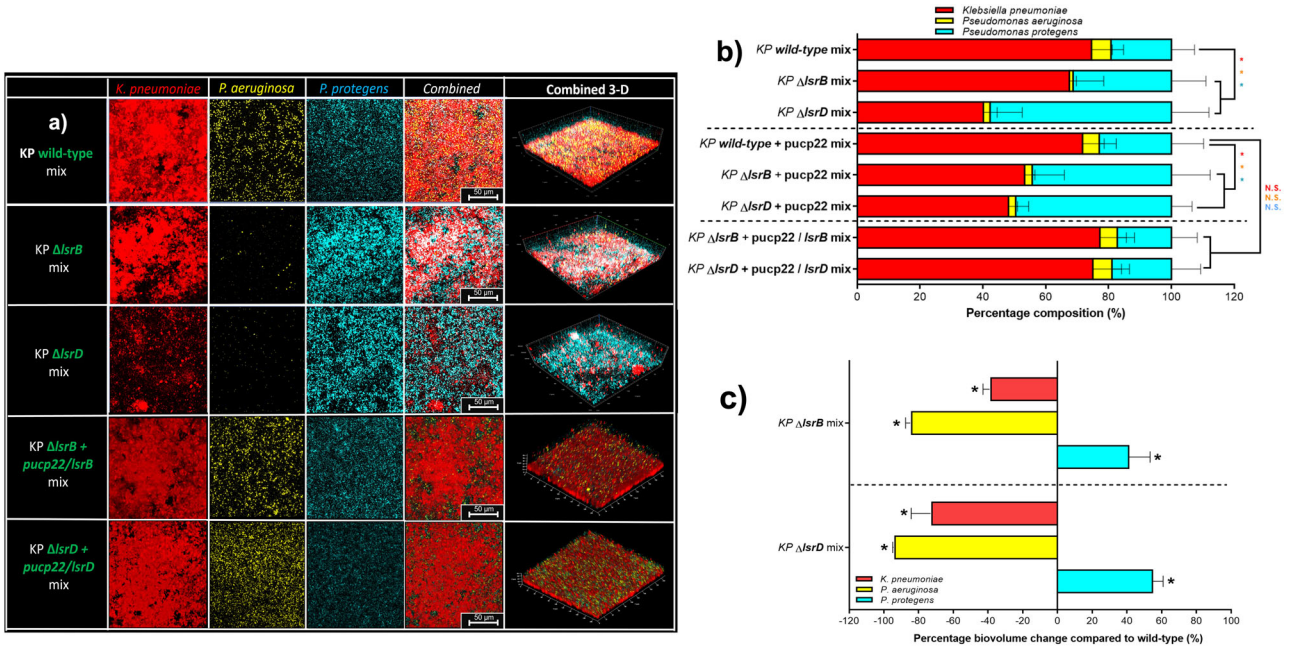

Fig. 3 | Three-species continuous-culture biofilms containing *K. pneumoniae* mutants and complemented mutants. a Representative CLSM images of biofilms consisting of *P. aeruginosa* (yellow), *P. protegens* (cyan) and *K. pneumoniae* (red) grown in M9CasGlucose. Scale bar is 50 μm. **b** Percent composition of mixed-species biofilms consisting of *P. aeruginosa*, *P. protegens* and *K. pneumoniae*. The *K. pneumoniae* strains used in the mixed-species biofilms were the wild-type, Δ*lsrB* and Δ*lsrD* (with or without the addition of pUCP22), as well as the complemented strains of the Δ*lsrB* and Δ*lsrD* deletion mutants (Δ*lsrB* + pUCP22/ *lsrB* and Δ*lsrD* + pUCP22/ *lsrD*, respectively). *P* values were determined by comparing the proportion of strain against the proportion of corresponding strain within mixed-species biofilms containing the wild-type *K. pneumoniae* (with or without the addition of the pUCP22 plasmid). Red, orange and blue asterisks (*) and "N.S." represent a significant difference ($P < 0.05$) and no significant difference in the proportions of *K. pneumoniae*, *P. aeruginosa* and *P. protegens*, respectively. **c** Percent change in biovolume of mixed-species biofilms containing Δ*lsrB* and Δ*lsrD* deletion mutants compared to mixed-species biofilms containing the wild-type *K. pneumoniae*. *P* values were determined by comparing biovolume of strain against the corresponding strain within the mixed-species biofilm containing the *K. pneumoniae* wild-type. The asterisk (*) denotes significant differences ($P < 0.05$), N.S. denotes no significant differences. $N = 9$ biological replicates, error bars represent standard deviation.

Changes in mixed-species biofilm composition upon deletion of *K. pneumoniae lsrB* and *lsrD* were due to the combined effect of individual interspecies interactions between *K. pneumoniae* and other members of the community

From the observations above, it was hypothesized that the effect of AI-2 transporters on community composition was facilitated by its effect on interspecies interactions within the community. To determine which pairwise interaction is responsible for driving the change in community composition within the three-species biofilm community, dual-species biofilms of *K. pneumoniae* + *P. aeruginosa* (Fig. 4) and K. *pneumoniae* + *P. protegens* (Fig. 5) were grown as continuous-culture biofilms over a 3-days period.

Dual-species biofilms of *K. pneumoniae* MGH78578 wild-type and *P. aeruginosa* formed two distinct layers, with *K. pneumoniae* occupying the top and growing over a layer of *P. aeruginosa* biofilm (Fig. 4a). When the *K. pneumoniae* wild-type was substituted with the Δ*lsrB* and Δ*lsrD* mutants, the distinct dual-layer of biofilms was disrupted and the dual-species biofilms adopted a more mixed spatial arrangement, with mixing occurring more in the dual-species biofilms containing the Δ*lsrD* mutant than in biofilms containing the Δ*lsrB* mutant (Fig. 4a). Complementation of *lsrB* and *lsrD* genes in the deletion mutants restored the wild-type dual-species biofilm arrangement (Fig. 4a). Apart from changes in spatial arrangement, deletion of *K. pneumoniae lsrB* and *lsrD* genes in the dual-species biofilms also resulted in significant changes in the composition of the dual-species biofilms. Substituting the wild-type *K. pneumoniae* with the Δ*lsrB* mutant resulted in a significant increase ($P < 0.001$) in the proportion of *K. pneumoniae* (69.5 ± 6.7% to 86.5 ± 5.4%) and a significant decrease ($P < 0.001$) in the proportion of *P. aeruginosa* (30.5 ± 8.2% to 13.5 ± 4.8%) (Fig. 4b). This change in proportion was associated with a non-significant decrease in the biovolume of *K. pneumoniae* (−3.2 ± 10.3%) and a significant decrease ($P < 0.001$) in the biovolume of *P. aeruginosa* (−64.6 ± 15.6%) (Fig. 4c). Likewise, the deletion of *lsrD* in the *K. pneumoniae* dual-species biofilm with *P. aeruginosa* resulted in a significant increase ($P < 0.001$) in the proportion of *K. pneumoniae* (69.5 ± 6.7% to 89.2 ± 6.9%) and a significant decrease ($P < 0.001$) in the proportion of *P. aeruginosa* (30.5 ± 6.7% to 10.8 ± 6.9%) (Fig. 4B). Consequently, there was a non-significant decrease in the biovolume of *K. pneumoniae* (−10.2 ± 11.5%) and a significant decrease ($P < 0.001$) in the biovolume of *P. aeruginosa* (−72.1 ± 21.8%) (Fig. 4c). When the wild-type and mutants of *K. pneumoniae* were transformed with pUCP22 plasmid, there was no significant changes in composition (Fig. 4b). Complementation of the Δ*lsrB* and Δ*lsrD* mutants resulted in dual-species biofilm proportions similar to the wild-type background strain (*K. pneumoniae* wild-type + pUCP22 with *P. aeruginosa*).

Unlike dual-species biofilms of *K. pneumoniae* and *P. aeruginosa*, dual-species biofilms of *K. pneumoniae* and *P. protegens* did not form two distinct layers, but rather adopted a more mixed spatial organization (Fig. 5a). Substitution of the wild-type *K. pneumoniae* with the Δ*lsrB* mutant resulted in a significant decrease ($P < 0.001$) in the proportion of *K. pneumoniae* (76.7 ± 3.8% to 58.0 ± 12.2%) and a significant increase ($P < 0.001$) in the proportion of *P. protegens* (23.3 ± 3.8% to 42.0 ± 12.2%) (Fig. 5b). This change in proportion was due to a significant decrease ($P < 0.001$) in the biovolume of *K. pneumoniae* (−44.9 ± 16.5%) and a significant increase ($P < 0.001$) in the biovolume of *P. protegens* (+44.1 ± 12.2%) (Fig. 5c). Similarly, dual-species biofilms formed by the *K. pneumoniae* Δ*lsrD* mutant had a significantly reduced ($P < 0.001$) proportion of *K. pneumoniae* (76.7 ± 3.8% to 41.5 ± 12.5%) and significantly increased ($P < 0.001$) proportion of *P. protegens* (23.3 ± 3.8% to 58.5 ± 12.5%) (Fig. 5b) compared to the dual-species biofilms formed by the wild-type. Accordingly, there was a

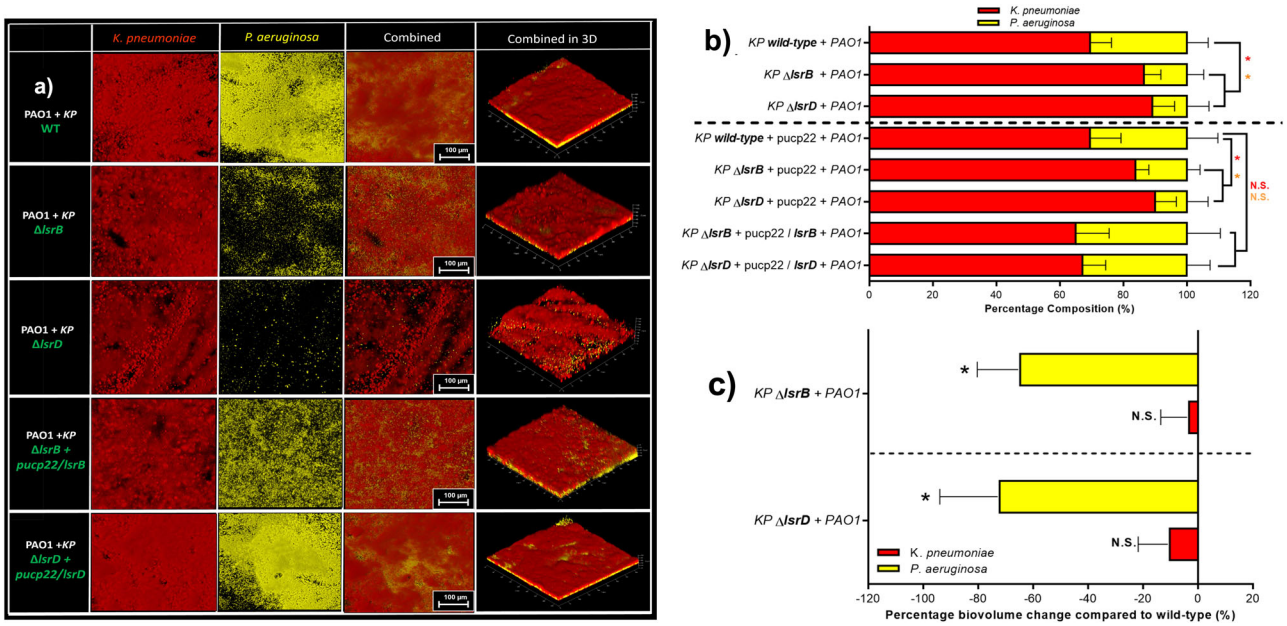

Fig. 4 | Dual-species continuous-culture biofilms containing *P. aeruginosa* grown with *K. pneumoniae* mutants and complemented strains. a Representative CLSM images of biofilms consisting of *P. aeruginosa* (yellow) and *K. pneumoniae* (red) grown in M9CasGlucose. Scale bar is 50 µm. **b** Percent composition of dual-species biofilms consisting of *P. aeruginosa* and *K. pneumoniae*. The *K. pneumoniae* strains used in the dual-species biofilms were the wild-type, Δ*lsrB* and Δ*lsrD* (with or without the addition of pUCP22), as well as the complemented strains of the Δ*lsrB* and Δ*lsrD* deletion mutant (Δ*lsrB* + pUCP22/ *lsrB* and Δ*lsrD* + pUCP22/ *lsrD*, respectively). *P* values were determined by comparing the proportion of strain against the proportion of corresponding strain within dual-species biofilms containing the wild-type *K. pneumoniae* (with or without the addition of pUCP22 plasmid). Red and orange asterisks (*) and "N.S" represent a significant difference ($P < 0.05$) and no significant difference in the proportions of *K. pneumoniae* and *P. aeruginosa*, respectively. **c** Percent change in biovolume of dual-species biofilms containing Δ*lsrB* and Δ*lsrD* deletion mutants compared to dual-species biofilms containing the wild-type *K. pneumoniae*. *P*-values were determined by comparing the biovolume of strain against the corresponding strain within the dual-species biofilm containing the *K. pneumoniae* wild-type. The asterisk (*) denotes a significant difference ($P < 0.001$), N.S. denotes no significant differences. $N = 3$ biological replicates, error bars represent standard deviation.

significant decrease ($P < 0.001$) in the biovolume of *K. pneumoniae* (−72.5 ± 10.0%) and a significant increase ($P < 0.001$) in the biovolume of *P. protegens* (+40.7 ± 11.9%) (Fig. 5c). Addition of the pUCP22 plasmid in the *K. pneumoniae* wild-type and Δ*lsrB* and Δ*lsrD* mutants did not significantly alter the composition of the dual-species biofilms with *P. protegens* (Fig. 5b). However, complementation of the *lsrB* and *lsrD* genes in the deletion mutants restored the dual-species biofilms to the wild-type phenotype.

Since complementation and fluorescence tagging in *K. pneumoniae* was carried out using plasmids, a plasmid retention assay was carried out to determine if plasmid loss could play a role in the compositional changes observed in mixed-species biofilms (Supplementary Fig. S1). After 72 h of planktonic growth, the percentage of *K. pneumoniae* colonies that lost the plasmid was ~5–10%, which was well within the range of standard deviation of the proportion of *K. pneumoniae* biomass within the mixed-species biofilm systems (Figs. 3–5).

AI-2 mediates interspecies interactions in planktonic cultures of *K. pneumoniae* and *P. aeruginosa*, but not *K. pneumoniae* and *P. protegens*

Dual-species, planktonic co-cultures of *P. aeruginosa*-*K. pneumoniae* (Fig. 6a) and P. *protegens*-*K. pneumoniae* (Fig. 6b) were competed to determine if the interspecies interactions observed in the mixed-species biofilms were biofilm-specific. Planktonic competition assays with *P. aeruginosa* and *K. pneumoniae* mutants showed that the interspecies interactions between the two were not biofilm-specific, with similar trends in percentage biofilm change in dual-species biofilms (Fig. 4b) and planktonic fitness (Fig. 6a). Substitution of the wild-type *K. pneumoniae* with Δ*lsrB* and Δ*lsrD* mutants resulted in significant decrease in the fitness of *P. aeruginosa* (−1.98 ± 0.51 and −0.88 ± 0.18, respectively) and a significant increase in the fitness of *K. pneumoniae* (+1.83 ± 0.18 and +1.17 ± 0.24, respectively). Replacing the Δ*lsrB* and Δ*lsrD* mutant strain with Δ*lsrB* and Δ*lsrD* + pUCP22 strains resulted in similar changes in planktonic fitness. When the Δ*lsrB* and Δ*lsrD* mutant strains were complemented, planktonic fitness of *K. pneumoniae* (+0.28 ± 0.08 and +0.21 ± 0.01, respectively) and *P. aeruginosa* (−0.26 ± 0.08 and −0.23 ± 0.12, respectively) were not significantly different compared to co-cultures containing the background strain (wild-type + pUCP22).

Planktonic competition assays with *P. protegens* and *K. pneumoniae* mutants (Fig. 6b) displayed different interactions than those in biofilms (Fig. 5b). Substitution of the wild-type *K. pneumoniae* with Δ*lsrB* and Δ*lsrD* mutants resulted in no significant changes in the fitness of *P. protegens* (+0.31 ± 0.02 and +0.17 ± 0.16, respectively) and in *K. pneumoniae* (−0.08 ± 0.16 and +0.24 ± 0.09, respectively). When *K. pneumoniae* Δ*lsrB* and Δ*lsrD* mutants were transformed with empty pUCP22 vectors and pUCP22 with *lsrB*/*lsrD* (complemented strains), planktonic fitness of *P. protegens* and *K. pneumoniae* did not display any significant changes compared to their respective wild-type background strains. Therefore, AI-2 transporters play a role in planktonic fitness between *P. aeruginosa* and *K. pneumoniae*, while AI-2 transporters do not mediate planktonic interactions between *P. protegens* and *K. pneumoniae*.

The addition of cell-free supernatants from *K. pneumoniae* deletion mutants did not result in the same changes in biofilm formation and planktonic growth in *P. aeruginosa* and *P. protegens*

To further elucidate the mechanism by which AI-2 produced by *K. pneumoniae* affects interspecies interactions, cell-free supernatants (CFS) of *K. pneumoniae* wild-type and deletion mutants were added to monospecies biofilms (Fig. 7) and planktonic cultures (Supplementary Fig. S2) of *P. aeruginosa* and *P. protegens*. CFS added to monospecies biofilms were either untreated or heat-treated and subjected to a size-exclusion filter

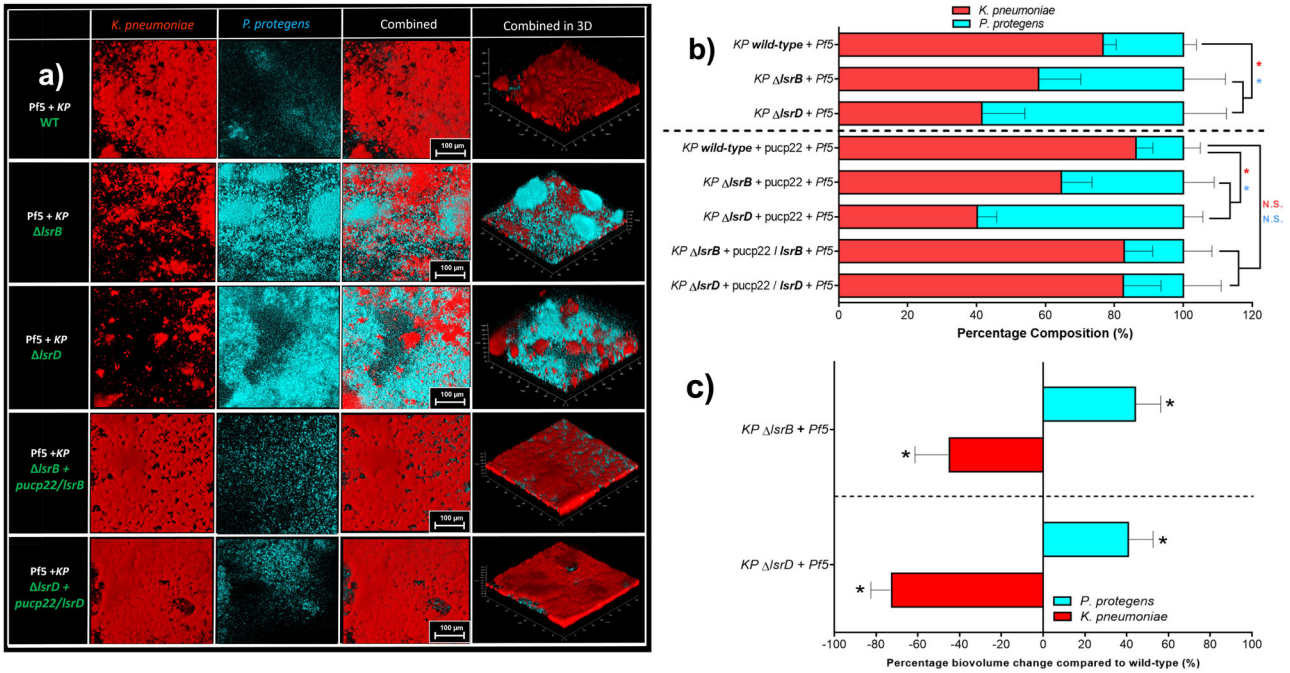

Fig. 5 | Dual-species continuous-culture biofilms containing *P. protegens* grown with *K. pneumoniae* mutants and complemented strains. a Representative CLSM images of biofilms consisting of *K. pneumoniae* (red) and *P. protegens* (cyan) grown in M9CasGlucose. Scale bar is 50 µm. **b** Percent composition of dual-species biofilms consisting of *K. pneumoniae* and *P. protegens*. The *K. pneumoniae* strains used in the dual-species biofilms were the wild-type, Δ*lsrB* and Δ*lsrD* (with or without the addition of pUCP22), as well as the complemented strains of the Δ*lsrB* and Δ*lsrD* deletion mutant (Δ*lsrB* + pUCP22/ *lsrB* and Δ*lsrD* + pUCP22/ *lsrD*, respectively). *P* values were determined by comparing the proportion of strain against the proportion of corresponding strain within dual-species biofilms containing the wild-type *K. pneumoniae* (with or without the addition of pUCP22 plasmid). Red and blue asterisks and "N.S." represent a significant difference ($P < 0.05$) and no significant difference in the proportions of *K. pneumoniae* and *P. protegens* respectively. **c** Percent change in biovolume of dual-species biofilms containing Δ*lsrB* and Δ*lsrD* deletion mutants compared to dual-species biofilms containing the wild-type *K. pneumoniae*. *P* values were determined by comparing biovolume of strain against the corresponding strain within the dual-species biofilm containing the *K. pneumoniae* wild-type. The asterisk (*) denotes significant difference ($P < 0.001$), N.S. denotes no significant differences. $N = 3$ biological replicates, error bars represent standard deviation.

(3 KDa) to remove secreted proteins and only retain small molecules such as AI-2. AI-2 has been shown to retain activity at 65 °C [35] and since it has a molecular size of 193.052 Da, it will not be removed from the CFS after being subjected to a size-exclusion filter with a cut-off of 3KDa. Unlike what was observed in dual-species biofilms (Fig. 4) and planktonic co-cultures (Fig. 6) of *K. pneumoniae* and *P. aeruginosa*, the addition of both treated and untreated CFS from *K. pneumoniae* Δ*lsrB* and Δ*lsrD* deletion mutants resulted in a significant increase ($P < 0.05$) in monospecies biofilm formation of *P. aeruginosa* compared to wild-type CFS (Fig. 7a). However, there were no significant differences in biomass of *P. protegens* monospecies biofilms when both treated and untreated CFS from *K. pneumoniae* Δ*lsrB* and Δ*lsrD* deletion mutants were added compared to the wild-type (Fig. 7b). Interestingly, the addition of CFS from *K. pneumoniae lsrB* and Δ*lsrD* deletion mutants did not result in an increased growth defect in the growth curves and growth rates of both planktonic cultures of *P. aeruginosa* and *P. protegens* compared to the wild-type *K. pneumoniae* CFS (Supplementary Fig. S2). These findings demonstrate that the AI-2 transporter-mediated interspecies interactions observed in both planktonic (Fig. 6) and biofilm (Figs. 3–5) systems were only present when *K. pneumoniae* is present within the system and is not purely the effect of AI-2 signal on *P. aeruginosa* and *P. protegens*.

Deletion of AI-2 transporters in *K. pneumoniae* results in a lower total biomass of biofilms in dual-species and three-species biofilms

To determine the effect the changes in composition had on the biomass of the dual-species and three-species biofilms, the total biovolume of the dual-species and mixed-species biofilms were quantified (Fig. 8). Three-species biofilms containing *K. pneumoniae* wild-type had a total biomass of $1.2 \times 10^7 \pm 2.3 \times 10^6$ µm^3, while three-species biofilms containing the *K. pneumoniae* Δ*lsrB* and Δ*lsrD* deletion mutants had a significantly lower ($P < 0.001$) biovolume of $8.5 \times 10^6 \pm 1.4 \times 10^6$ µm^3 and $6.9 \times 10^6 \pm 1.8 \times 10^6$ µm^3, respectively (Fig. 8a). This trend was also observed in dual-species biofilms containing *K. pneumoniae*. In dual-species biofilms comprised of *K. pneumoniae* and *P. aeruginosa*, substituting the wild-type *K. pneumoniae* with Δ*lsrB* and Δ*lsrD* deletion mutants resulted in a significant decrease ($P < 0.001$) in biomass from $1.0 \times 10^7 \pm 2.0 \times 10^6$ µm^3 to $7.8 \times 10^6 \pm 1.4 \times 10^6$ µm^3 and $7.1 \times 10^6 \pm 1.6 \times 10^6$ µm^3, respectively (Fig. 8b). Similarly, in dual-species biofilms composing of *K. pneumoniae* and *P. protegens*, deletion of *lsrB* and *lsrD* resulted in a significant reduction ($P < 0.001$) in biomass, from $1.2 \times 10^7 \pm 2.8 \times 10^6$ µm^3 to $9.2 \times 10^6 \pm 1.6 \times 10^6$ µm^3 and $6.5 \times 10^6 \pm 1.1 \times 10^6$ µm^3, respectively. This data demonstrates that the ability for *K. pneumoniae* to transport AI-2 back into the cell is important for the mixed-species biofilms to achieve maximum biofilm biomass.

Discussion

Microbes in nature typically exist in multispecies biofilms where interspecies interactions define the spatial organization and composition of member species. This contrasts with planktonic communities or monospecies biofilms, which lack the co-operative or competitive interactions that arise within multispecies biofilms and that typically result in the emergence of community-level properties[11,36–38]. These interactions are controlled by genes and signals from various species that interact with one another, ultimately reaching a compositional equilibrium within the mixed-species biofilm. In this study, the deletions in two genes involved in AI-2 transport in *K. pneumoniae*, *lsrB* and *lsrD*, were investigated to understand their role in mediating monospecies biofilm formation, as well as their impacts on the

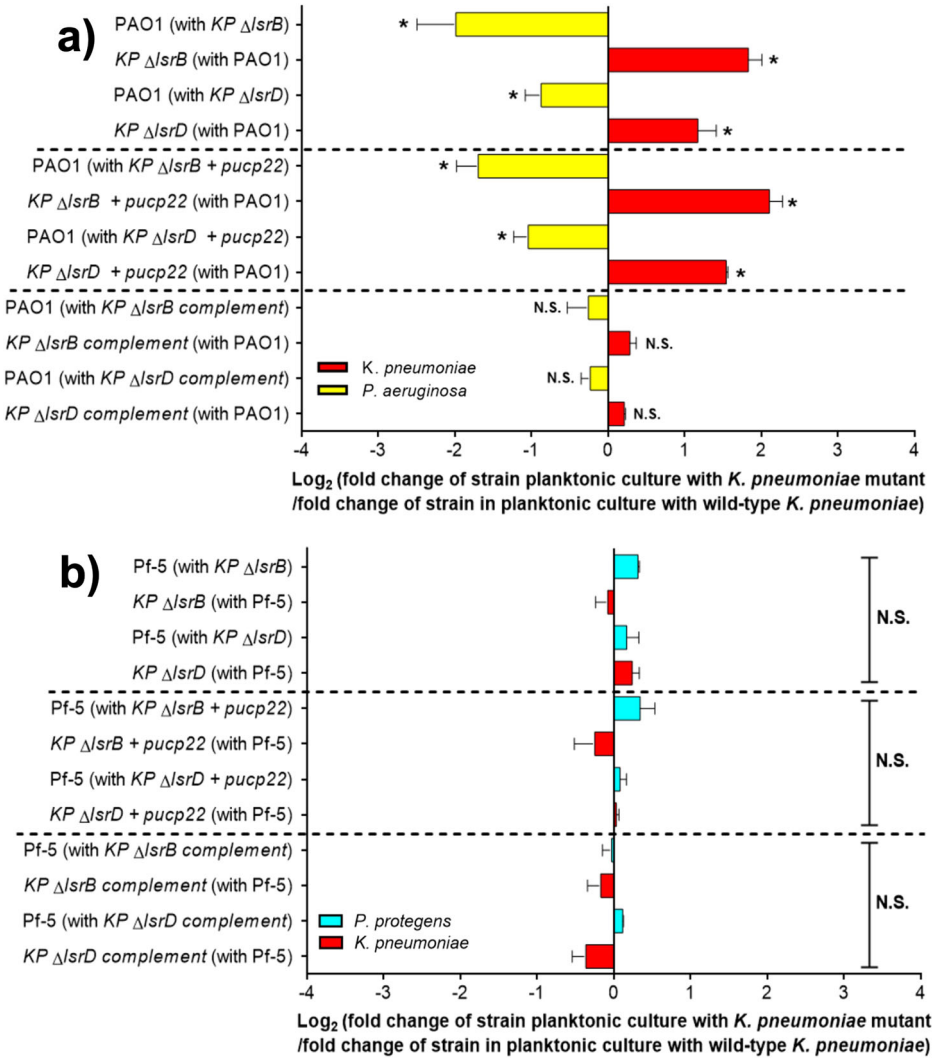

Fig. 6 | Dual-species fitness assays with *K. pneumoniae* mutants and complemented strains. Competitive fitness assays of *K. pneumonia* wild-type (with or without pUCP22), Δ*lsrB* and Δ*lsrD* deletion mutants (with or without pUCP22) and Δ*lsrB* and Δ*lsrD* complemented strains grown as planktonic cultures with **a** *P. aeruginosa* or **b** *P. protegens*. The two species were inoculated at a 1:1 ratio and grown for 24 h. CFU of the cultures were counted at 0 and 24 h, and fitness was plotted as Log_2[Fold change of strain grown in co-culture containing *K. pneumoniae* mutant or complement/ fold change of strain grown in co-culture containing *K. pneumoniae* wild-type. Yellow, red and cyan bars indicate the fitness of *P. aeruginosa*, *K. pneumoniae*, and *P. protegens*, respectively. *P* values were calculated by comparing the fold change of CFU in the mutant/complement strain with the fold change of CFU in corresponding wild-type background strain. $N = 3$ biological replicates. The asterisk (*) denotes significant difference ($P < 0.05$), N.S. denotes no significant differences, and error bars represent standard deviation.

composition and organization of a three-species experimental biofilm model consisting of *K. pneumoniae* MGH78578, *P. aeruginosa* PAO1, and *P. protegens* Pf-5.

Deletion in *lsrB* and *lsrD* resulted in a significant increase in the extracellular concentration of AI-2, presumably through reduced ability to recognize, bind and internalize the AI-2 signals. This observation was consistent with the current understanding on the role of the *lsrB* and *lsrD* genes in AI-2 transport, where deletion of *lsrB* and *lsrD* genes in *E. coli* resulted in increased extracellular AI-2 levels[39]. Interestingly, the decrease in AI-2 internalization within the *K. pneumoniae* Δ*lsrB* mutants was only observed in the early stages of biofilm formation in both batch cultures but was not significantly different to the wild-type at later stages of biofilm formation (Fig. 1c, d). This could be due to the presence of a secondary mode of AI-2 transport in *K. pneumoniae*, such as the *rbsDABCK* operon, which has been demonstrated to encode a secondary AI-2 transporter in *Aggregatibacter actinomycetemcomitans* and non-typeable *Haemophilus influenzae*, which allowed mutants defective in Lsr transporter to still internalize AI-2[40,41]. In the same study, the alternative receptor, RbsB exhibited lower efficiency in AI-2 uptake compared to the cognate LsrB receptor in *A. actinomycetemcomitans*[41]. This observation could explain the differences in extracellular AI-2 levels in the early and late-stage biofilms formed by the *K. pneumoniae* mutants.

The deletion of *lsrB* and *lsrD* genes in *K. pneumoniae* did not result in significant changes in growth rate nor in monospecies biofilm formation when grown in M9 medium (Fig. 2a–e). The role of AI-2 QS in biofilm formation of *K. pneumoniae* is not clearly defined, and varies depending on the strain of *K. pneumoniae*, experimental set-up, and medium used[42]. For example, deletion in *lsrB* in *E. coli* resulted in a decrease in AI-2 dependent autoaggregation and batch biofilm formation when grown in LB medium[25]. However, when the *lsrB* and *lsrD* genes were deleted in *K. pneumoniae* LM21, the mutants formed biofilms with larger surface area, but with lowered thickness when grown on M63B1-0.4% Glu medium at 37 °C on Thermanox slides in a microfermentor system[43]. In this study, deletion of *lsrB* and *lsrD* in *K. pneumoniae* MGH78578 did not lead to significant changes biofilm formation when grown as monospecies batch biofilms or continuous-culture biofilms in M9CasGlucose. Furthermore, auto-aggregation in *K. pneumoniae* was unaffected upon deletion of both *lsrB* and *lsrD* (Fig. 2f). Since autoaggregation and biofilm formation are typical phenotypes associated with AI-2 signaling[19,25], the observation that *K. pneumoniae* Δ*lsrB* and Δ*lsrD* mutants did not display any differences in autoaggregation and biofilm further suggests that AI-2 signaling still could proceed even without these two genes.

Furthermore, the role of these genes in mediating interspecies interactions with *P. aeruginosa* and *P. protegens* in planktonic and biofilm cultures were investigated (Table 1). Deletion of *lsrB* and *lsrD* resulted in *K. pneumoniae* being more effective in outcompeting *P. aeruginosa* than the wild-type, and this interaction was observed in both planktonic cultures (Fig. 6a) and in dual-species biofilms (Fig. 4b, c). Furthermore, substituting the wild-type *K. pneumoniae* with the Δ*lsrB* and Δ*lsrD* mutant disrupted the dual-biofilm layer in the

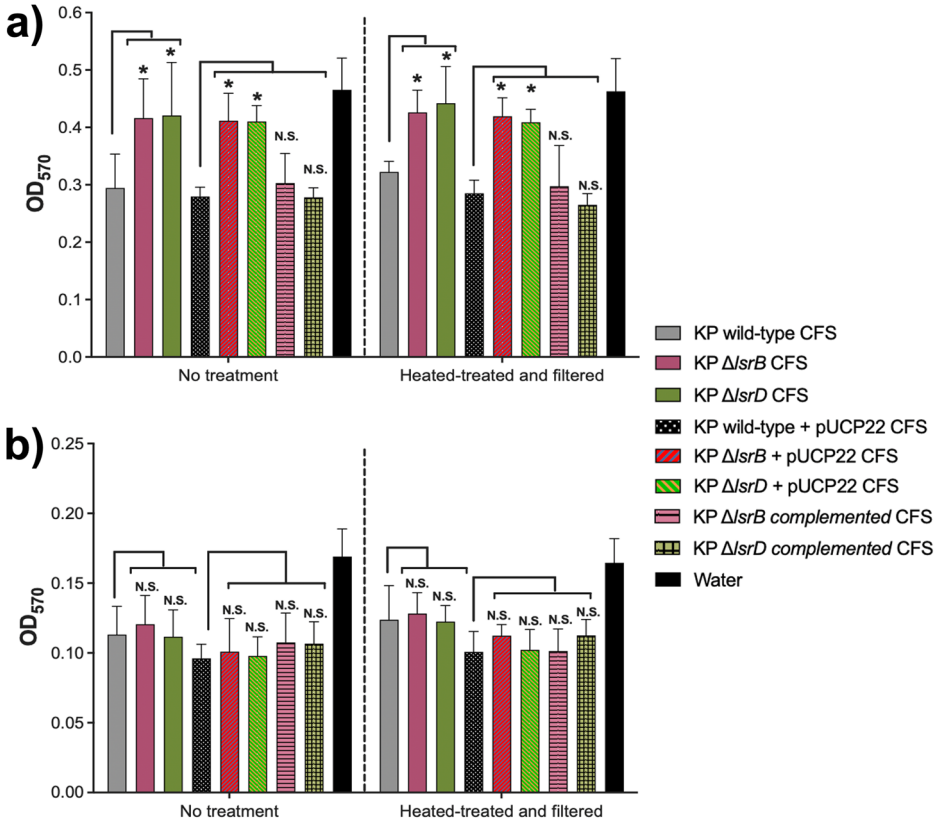

Fig. 7 | Batch biofilm formation after the addition of cell-free supernatants (CFS) from *K. pneumoniae*. Crystal violet assay quantifying biofilm formation of **a** *P. aeruginosa* PAO1 and **b** *P. protegens* Pf5 when cell-free supernatants from various *K. pneumoniae* strains were added. Cell-free supernatants of a 12 h culture of *K. pneumoniae* were either added without any treatment (untreated CFS) or heat-treated and subjected to filtration with molecular weight cut-off of 3 kDa to remove secreted proteins (heat-treated and filtered CFS). Sterile deionized water was added as a negative control. $N = 3$ biological replicates. The asterisk (*) denotes significant difference ($P < 0.05$), N.S. denotes no significant differences, and error bars represent standard deviation.

continuous-culture biofilm flow chambers (Fig. 4a). The biofilm layering as observed for the wild-type *K. pneumoniae* and *P. aeruginosa* is indicative of a co-operative interaction between the two species[44,45]. This suggests that the loss of the AI-2 transporter system in *K. pneumoniae* resulted in a change in interspecies interactions with *P. aeruginosa* from co-operative to competitive. It is conceivable that this observed effect was due to the increased levels of extracellular AI-2 resulting in an inhibition of *P. aeruginosa* planktonic growth and biofilm formation. Previous reports have established that purified AI-2 signals affect *P. aeruginosa* biofilm formation through the effects of AI-2 on AHL-mediated QS. The addition of purified AI-2 of a concentration up to 10 nM resulted in an increase in biofilm formation and colonization in mice lungs in *P. aeruginosa* PAO1, through an increase in the expression of QS effectors[30,31]. Moreover, a distinct AI-2 receptor was discovered in *P. aeruginosa* which could allow it to respond to AI-2 signals[46]. However, previous studies only investigated the effect of chemically synthesized AI-2 on *P. aeruginosa*, and not the potential changes in interspecies interactions it could have on other species as a result of increased extracellular AI-2 secretion by an AI-2 secreting species. Since a decrease in fitness in *P. aeruginosa* was also observed in planktonic cultures, it is unlikely that the decrease in biofilm formation observed in dual-species biofilms with *K. pneumoniae* was as a result of a AI-2 mediated decrease in biofilm formation in *P. aeruginosa*. Instead, it is more likely that the increase in extracellular AI-2 resulted in changes in expression of *P. aeruginosa* genes which led to it being outcompeted more by *K. pneumoniae* mutants in planktonic and dual-species biofilm cultures. For example, *P. aeruginosa* could respond to increased extracellular AI-2 by down-regulating its Type VI secretion (T6SS) genes or QS-specific genes involved in competition, such as rhamnolipids or other metabolic genes. AI-2 secretion by one species have been shown to affect interspecies competition in previous studies. For example, AI-2 signals generated from *Photorhabdus luminescens* resulted in a 50% reduction in the biofilm formation of *Bacillus cereus* through induction of dispersal of cells from preformed biofilm[47]. In addition, the addition of AI-2 into *Desulfovibrio sp.* resulted in significantly lowered biofilm formation through reduction of EPS within the biofilm[48].

When *K. pneumoniae* was competed against *P. protegens*, deletion of *lsrB* and *lsrD* resulted in *P. protegens* outcompeting the *K. pneumoniae* mutants more than when the wild-type was present. This interaction in dual-species biofilms was a result of an increase in the biofilm formation of *P. protegens* and a decrease in biofilm formation of *K. pneumoniae* (Fig. 5c). However, when these two species competed in planktonic cultures, the trends in competitive index observed in the dual-species biofilms were not similarly observed. This suggests that the loss of the AI-2 transporter system, and the concomitant increase in extracellular AI-2, resulted in biofilm-specific increase in fitness in *P. protegens*. AI-2 secretion from a single species within a biofilm consortium have been demonstrated to have positive effects on neighboring species. For example, secretion of AI-2 from *Fusobacterium nucleatum* resulted in increased biofilm formation of three other periodontal bacteria species in a multispecies biofilm model[49]. Similarly, AI-2 secretion from *K. pneumoniae* seemed to induce biofilm formation of *P. protegens* while inhibiting the growth and biofilm formation of *P. aeruginosa*, thereby acting as "bridge organism" within the three-species biofilm community. similar to *F. nucleatum* within the periodontic bacteria community[49].

The mechanism by which AI-2 modulate interspecies interactions was further elucidated through biofilm and growth rate assays with the addition of cell-free supernatants from *K. pneumoniae* (Fig. 7 and Supplementary Fig. S2). *P. aeruginosa* and *P. protegens* cultured with CFS from *K. pneumoniae*, in the absence of *K. pneumoniae*, did not reproduce the same interspecies interactions observed in the mixed-species biofilms (Figs. 3–5) and planktonic co-cultures (Fig. 6). For example, while deletion of *lsrB* and *lsrD* resulted in a decrease in biofilm formation in *P. aeruginosa* in dual-species biofilms (Fig. 4), addition of CFS from the same mutants resulted in an increase in monospecies biofilm formation of *P. aeruginosa* (Fig. 7). Previous studies have demonstrated that the addition of chemically

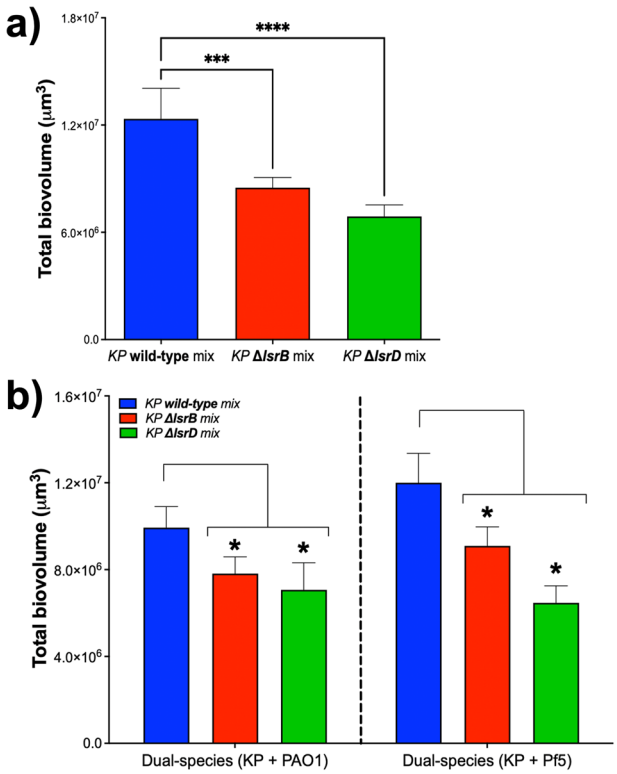

Fig. 8 | Total biomass of mixed-species and dual-species biofilms. Comparison of total biomass of **a** three-species biofilms (*K. pneumoniae* + *P. aeruginosa* + *P. protegens*) and **b** dual-species biofilms (*K. pneumoniae* + *P. aeruginosa* and *K. pneumoniae* + *P. protegens*) when *K. pneumoniae* wild-type and Δ*lsrB* and Δ*lsrD* deletion mutants were present in the mixed-species biofilms. *P* values were calculated by comparing the total biovolume of all two/three strains in biofilms containing *K. pneumoniae* wild-type to biofilms containing *the K. pneumoniae* Δ*lsrB* and Δ*lsrD* deletion mutants. The asterisk (*) denotes significant difference ($P < 0.001$), N.S. denotes no significant differences. $N = 9$ biological replicates for (**a**) and $N = 3$ biological replicates for (**b**). Error bars represent standard deviation.

synthesized AI-2 resulted in an increase in biofilm formation in *P. aeruginosa* through the action of AHL-based QS[30,31]. This observation was consistent with what was observed in this study, where biofilm formation of *P. aeruginosa* increased when CFS from *K. pneumoniae* (which contains AI-2 at physiologically relevant conditions) was added in this study (Fig. 7). Similarly, while the planktonic fitness of *P. aeruginosa* decreased when co-cultured with *K. pneumoniae lsrB* and *lsrD* deletion mutants (Fig. 6), the same observation was not reproduced when CFS from *K. pneumoniae* was introduced into planktonic cultures of *P. aeruginosa* (Supplementary Fig. S2). These findings indicate that the AI-2-mediated interspecies interactions observed in mixed-species biofilms are only when *K. pneumoniae* is present in the community and is not solely due to the effect of AI-2 signaling molecule on *P. aeruginosa* and *P. protegens* in isolation. Likely, the increase in extracellular AI-2 in the mixed-species biofilm community resulted in changes in interspecies interactions between *K. pneumoniae* and other members of the community, resulting in changes in community composition. This is further evidence that the presence of *K. pneumoniae* within the mixed-species community serves as a "bridging organism", which mediates interspecies interactions between itself and other members of the community through the action of AI-2. In addition, as mentioned above, the biofilm growth response of *P. aeruginosa* and *P. protegens* to AI-2 secreted by *K. pneumoniae* in dual-species biofilms was different, with former being inhibited and the latter being promoted by AI-2. This opposing effect of AI-2 on different species have been observed before. In a previous study, *F. nucleatum* promoted the biofilm formation of *S. gordonii*, but within the same system, inhibited the biofilm growth of *Streptococcus oralis*[50]. However, in that study, the secreted AI-2 from the cell-free supernatant of *F. nucleatum* also had the same effect on the biofilm formation of *S. gordonii* and *S. oralis*, while this was not the case in this study. Interestingly, the authors also reported a decrease in the biofilm formation of *F. nucleatum* through the decrease in attachment to preformed *S. gordonii* biofilm[50]. Previous studies have shown that *K. pneumoniae* biofilm grows on top of a base biofilm of *P. aeruginosa*[51]. This spatial organization of dual-species biofilms of *K. pneumoniae* and *P. aeruginosa* was also observed in this study (Fig. 4a). Therefore, it is possible that the AI-2 mediated decrease in biofilm formation in *K. pneumoniae* in dual-species biofilm with *P. aeruginosa* (Fig. 4c) was due to there being a lower volume of basal *P. aeruginosa* biofilm for *K. pneumoniae* to attach to and mature on. This could explain why there

Table 1 | Summary of the changes in planktonic fitness or in composition of biofilms in the *K. pneumoniae* mutants compared to the wild-type

	K. pneumoniae	*P. aeruginosa*	*P. protegens*
Planktonic (*K. pneumoniae* Δ*lsrB* + *P. aeruginosa*)	*Fitness* ↑	*Fitness* ↓	
Planktonic (*K. pneumoniae* Δ*lsrD* + *P. aeruginosa*)	*Fitness* ↑	*Fitness* ↓	
Planktonic (*K. pneumoniae* Δ*lsrB* + *P. protegens*)	*Fitness* —(N.S.)		*Fitness* —(N.S.)
Planktonic (*K. pneumoniae* Δ*lsrD* + *P. protegens*)	*Fitness* —(N.S.)		*Fitness*—(N.S.)
Dual-species biofilm (continuous-culture) (*K. pneumoniae* Δ*lsrB* + *P. aeruginosa*)	*Proportion* ↑ (*)*Biovolume* —(N.S.)	*Proportion* ↓ (*)*Biovolume* ↓ (*)	
Dual-species biofilm (continuous-culture) (*K. pneumoniae* Δ*lsrD* + *P. aeruginosa*)	*Proportion* ↑ (*)*Biovolume* —(N.S.)	*Proportion* ↓ (*)*Biovolume* ↓ (*)	
Dual-species biofilm (continuous-culture) (*K. pneumoniae* Δ*lsrB* + *P. protegens*)	*Proportion* ↓ (*)*Biovolume* ↓ (*)		*Proportion* ↑ (*)*Biovolume* ↑ (*)
Dual-species biofilm (continuous-culture) (*K. pneumoniae* Δ*lsrD* + *P. protegens*)	*Proportion* ↓ (*)*Biovolume* ↓ (*)		*Proportion* ↑ (*)*Biovolume* ↑ (*)
Mixed-species biofilm (continuous-culture) (*K. pneumoniae* Δ*lsrB* + *P. aeruginosa* + *P. protegens*)	*Proportion* ↓ (*)*Biovolume* ↓ (*)	*Proportion* ↓ (*)*Biovolume* ↓ (*)	*Proportion* ↑ (*)*Biovolume* ↑ (*)
Mixed-species biofilm (continuous-culture) (*K. pneumoniae* Δ*lsrD* + *P. aeruginosa* + *P. protegens*)	*Proportion* ↓ (*)*Biovolume* ↓ (*)	*Proportion* ↓ (*)*Biovolume* ↓ (*)	*Proportion* ↑ (*)*Biovolume* ↑ (*)

The (–) symbol denotes a non-significant change in quantity compared to the wild-type. The (↓) symbol denotes a significant decrease in quantity compared to the wild-type. The (↑) symbol denotes a significant increase in quantity compared to the wild-type. The (N.S.) symbol denotes no significant change. The asterisk (*) denotes a significant change ($P < 0.05$) after ANOVA or *t* test.

was a decrease in the biovolume of both *P. aeruginosa* and *K. pneumoniae* in dual-species biofilms (Fig. 4c) and a similar decrease in three-species biofilm (Fig. 3c), even when there was an increase in the fitness of *K. pneumoniae* in planktonic culture (Fig. 6).

The changes in composition within the three-species biofilm was observed to be due to the cumulative effects of individual pairwise interactions of *P. protegens* and *P. aeruginosa* with the *K. pneumoniae* Δ*lsrB* and Δ*lsrD* mutants (Table 1). Thus, the AI-2 mediated increase in biomass of *P. protegens* in the three-species community was due to the pairwise interspecies interactions between *K. pneumoniae* and *P. protegens* (Table 1). Similarly, the decrease in biomass of *P. aeruginosa* in the three-species community was as a result of interspecies competition between *K. pneumoniae* and *P. aeruginosa* (Table 1). Furthermore, the AI-2-mediated decrease in the biomass of *K. pneumoniae* in the three-species biofilm was as a result of competition between *K. pneumoniae* and *P. protegens*, and not as a result of the dual-species interactions with *P. aeruginosa*. Therefore, these pairwise interactions involving AI-2 secreted by the bridging organism *K. pneumoniae* mediates the composition of the entire biofilm and is important for maintaining the compositional equilibrium within the biofilm consortium.

The changes in community composition in both dual and three-species biofilms resulted in a significant decrease in the total biomass of biofilm (Fig. 8). This suggests that the ability of *K. pneumoniae* to take up AI-2 is crucial in maintaining the optimal three-species community composition of ~80% *K. pneumoniae*, 15% *P. protegens* and 5% *P. aeruginosa*. This composition was consistently reached after 3 days of growth in this study as well as in previous studies using this three-species biofilm model[11,14,15]. For example, a previous study showed that polysaccharides produced by *P. aeruginosa* confer SDS resistance to the three-species biofilm community[14]. In addition, *P. protegens* was also observed to confer tobramycin resistance to the three-species biofilm community[11]. In the same study, it was also observed that the composition of the three-species biofilm community was different at the inlet and outlet of the flow cell, suggesting that different nutritional environments can influence the composition of the community, possibly due to the biofilm adapting the composition to favor more efficient metabolite exchange[11]. These observations suggest that an optimal compositional equilibrium could allow for the most beneficial exchange of metabolites or conferring the maximum level of resilience, and disruption of this equilibrium could result in non-optimal biofilm growing conditions. The ability of a QS system within a member of the community to mediate interactions and community composition was also observed in a previous study performed in our laboratory[15]. In that study, AHL-mediated QS in *P. aeruginosa* resulted in changes in community composition by modulating competition against *P. protegens*. This shows that QS in both *P. aeruginosa* (~5% biomass) and *K. pneumoniae* (~80% biomass) mediate interspecies interactions and therefore, community composition.

Although the increase in extracellular AI-2 upon deletion of *lsrB* and *lsrD* genes could have resulted in the observations made above, there remains other possibilities. Instead of the direct effects of the AI-2 molecule on *P. aeruginosa* and *P. protegens*, the changes in interspecies interactions could also have resulted from the disruption of AI-2 QS signaling in *K. pneumoniae* itself. However, this is unlikely due two main reasons. First, the AI-2 assay performed on the *K. pneumoniae* Δ*lsrB* mutant demonstrated that extracellular AI-2 was only higher compared to the wild-type only in the early stages of biofilm formation, while the *K. pneumoniae* Δ*lsrD* mutant displayed decreasing extracellular AI-2 over time (Fig. 1c, d). This suggests that the AI-2 is still being internalized in both the *K. pneumoniae* Δ*lsrB* and Δ*lsrB* mutants, albeit at a lower efficiency than the wild-type, therefore potentially still allowing for QS signaling. Second, the phenotypes which are usually associated with a disruption in AI-2 QS signaling, such as monospecies biofilm formation and aggregation[25], were not significantly different in the *K. pneumoniae* Δ*lsrB* and Δ*lsrB* mutants compared to the wild-type (Fig. 2c–f). This suggests that the AI-2 QS signaling pathways in *K. pneumoniae* were not substantially affected by the deletion of *lsrB* and *lsrD*.

In addition, there were observed differences in competition when biofilms of *K. pneumoniae* Δ*lsrB* and *K. pneumoniae* Δ*lsrD* mutants were grown as mixed-species biofilms. Changes in proportion and biomass of mixed-species biofilms containing *K. pneumoniae* Δ*lsrD* mutants occurs at a greater degree than when *K. pneumoniae* Δ*lsrB* mutants was present (Figs. 3–5 and 8). This can be explained by the observation that extracellular AI-2 remains high in *K. pneumoniae* Δ*lsrD* mutant biofilms and was lower in the *K. pneumoniae* Δ*lsrB* mutant biofilms after 24 h of growth (Fig. 1c, d). Since mixed-species biofilms were cultured for longer than 24 h (72 h), the maintenance of high levels of AI-2 in *K. pneumoniae* Δ*lsrD* over long periods of time could have resulted in larger changes in proportion in mixed-species biofilms. This observation is further evidence that extracellular AI-2 is the main driver of compositional change in mixed-species biofilms when AI-2 transporters in *K. pneumoniae* was deleted. However, this same observation was not seen in planktonic competition assays (Fig. 6a), where the changes in fitness in *K. pneumoniae* and *P. aeruginosa* was larger when *lsrB* was deleted instead of *lsrD*. This suggests that under planktonic conditions, sensing of AI-2 signals (LsrB) by *K. pneumoniae* could play a larger role in competition with *P. aeruginosa* than the extracellular transport of AI-2. The sensing of AI-2 by LsrB have been shown to mediate collective behavior such as virulence, chemotaxis and aggregation, all of which could have played a role in planktonic competition[25].

In conclusion, *lsrB* and *lsrD* in *K. pneumoniae* were determined to have an important role in mediating interspecies interactions in multispecies biofilms with *P. aeruginosa* and *P. protegens*. The change in composition in the three-species biofilm was as a result of the additive effects on individual dual-species interactions in *K. pneumoniae* with *P. aeruginosa* and *P. protegens*. It was likely that the differences in interspecies interactions upon deletion of *lsrB* and *lsrD* were as a result of the increase in extracellular AI-2 concentration, which resulted in changes in gene expression in *P. aeruginosa* and *P. protegens*, leading to changes in competition or metabolism in the mixed-species biofilms. Future studies can be performed to determine the exact mechanisms by which the impairment of AI-2 uptake by *K. pneumoniae* results in changes in interspecies interactions and composition of multispecies biofilms. In addition, future studies could further investigate the mechanism of action of AI-2 on the opposing effects on competition between *K. pneumoniae* and *P. aeruginosa* and between *K. pneumoniae* and *P. protegens*. The findings in this study advances the understanding of interspecies interactions within mixed-species biofilms and could lead to solutions on combating harmful mixed-species biofilms in nature or unlock the potential of mixed-species biofilms in various applications throughout multiple industries.

Methods

Bacterial strains and media

Bacterial strains (Table 2) were cultured in M9CasGlucose minimal medium (48 mM Na_2HPO_4; 9 mM NaCl; 22 mM KH_2PO_4; 19 mM NH_4Cl; 0.1 mM $CaCl_2$; 2 mM $MgSO_4$; 0.04% w/v glucose; 0.2% w/v casamino acids), Autoinducer Bioassay Medium (1.75% w/v NaCl, 0.085 M $MgSO_4$, 0.2% w/v Casamino acids, 0.01 M K_3PO_4, 0.001 M L-arginine, 1% glycerol) or Lysogeny Broth (Lennox and Miller). Gentamicin (30 ng/μl), hygromycin (100 ng/μl) and apramycin (50 ng/μl) (MP Biomedicals, Singapore) were used as needed. The eYFP-tagged *P. aeruginosa* PAO1 (ATCC BAA-47) and eCFP-tagged *P. protegens* PF-5 (ATCC BAA-477) were previously generated in our laboratory[15]. The mCherry-tagged *K. pneumoniae* MGH78578 deletion mutants were generated in this study.

Generation of fluorescently tagged gene deletion mutants of *K. pneumoniae*

The protocol for the deletion of *K. pneumoniae* MGH78578 genes (*lsrB* and *lsrD*) was modified and adapted from a previous study[52]. A single colony of *K. pneumoniae* MGH78578 was inoculated into 5 ml LB medium and grown at 37 °C overnight. A 1 ml aliquot of overnight culture was added into 100 ml of fresh LB medium and incubated at 37 °C with shaking for approximately 4 h (OD_{600} of 0.4–0.6) and made electrocompetent using ice-

Table 2 | List of bacterial strains used

Species and strains	Phenotype	Fluorescent tag	Source/reference
P. aeruginosa (PAO1)	Wild type	eYFP	(ATCC BAA-47)[a][15]
P. protegens (Pf-5)	Wild type	eCFP	(ATCC BAA-477)[a][15]
K. pneumoniae (MGH78578)	Wild type	mCherry	(ATCC 700721)[a]
K. pneumoniae (MGH78578Δ*lsrB*)	LsrB autoinducer-2 transporter protein deletion mutant	mCherry	This study
K. pneumoniae (MGH78578 Δ*lsrD*)	LsrD autoinducer-2 transporter protein deletion mutant	mCherry	This study
Vibrio harveyi BB170	AI-1 sensor negative, AI-2 sensor positive	-	(ATCC BAA-1117)[a][18]

[a]American Type Culture Collection (ATCC) number.

Table 3 | List of plasmids used for generating mutants and complementation constructs

Plasmid name	Characteristics	Reference
pACBSR-hyg	Hyg^R; modified pBAD vector expressing lambda-red system	52
pFLP-hyg	Hyg^R; modified pCP20 vector expressing FLP recombinase	52
pMDIAI	Amp^R; modified pMD18-T simple backbone vector with a portion derived from pIJ773 [57]. Plasmid is used as a template for amplifying gene sequence flanked Apramycin resistance cassette	52
pFA6a-mCherry-hphMX6	Hyg^R; modified pFA6a vector expressing mCherry fluorescent protein	56
pUCP22notI	$Gent^R$; Pseudomonas sp.- *Escherichia coli* shuttle plasmid	57

cold glycerol. The culture was first centrifuged for 5 min at 7000 × *g* and the cell pellet was resuspended in 50 ml 10% ice-cold glycerol. This process was further repeated three times. After the final wash, the pellet was resuspended in 500 µl of 10% ice-cold glycerol to obtain electrocompetent *K. pneumoniae* MGH78578. The plasmid pABSCR-hyg (Table 3), which contains genes that facilitate recombination, was transformed into the electrocompetent *K. pneumoniae*. This was achieved by adding 400 ng of pACBSR-hyg to 50 µl of electrocompetent *K. pneumoniae* suspended in ice-cold glycerol and transferring this mixture into a cold electroporation cuvette (2 mm gap). Transformation (25 mF, 200 W, 5 ms pulse time and 2 kV/cm) was carried out using a Gene Pulsar Electroporator (Biorad, Hercules, CA, USA). Two hundred fifty microliters of pre-warmed (37 °C) SOC medium (Thermo Fisher Scientific, MA, USA) was added to the transformed cells and this mixture was incubated with shaking for 1 h at 30 °C. Successful transformants were selected by plating on LB plates with 50 ng/µl hygromycin and incubated for 30 °C overnight.

A knockout cassette was generated by amplifying an FRT-flanked ApraR cassette from the pMDIAI plasmid (Supplementary Table S1, primers used) with overlapping arms homologous to the gene of interest to be deleted. PCR was carried out with the following conditions: 98 °C initial denaturation step (30 s), 35 cycles of 98 °C denaturation (10 s), 55–70 °C annealing (30 s), and 72 °C extension (45 s) and a final extension step of 72 °C (120 s). The PCR-amplified knockout cassette was then transformed into pABSCR-positive *K. pneumoniae* colonies following the same transformation protocol as mentioned above and successful homologous recombination was selected by LB plates containing 50 ng/µl apramycin. The resulting colonies were screened for correct insertion of knockout cassette by PCR amplification and sequencing using confirmation sequencing primers (Supplementary Table S1) and the same PCR settings as above. Colonies with the correct inserts were further screened for loss of the pABSCR-hyg plasmid by streaking onto LB Apramycin and LB Hygromycin plates and incubated at 37 °C overnight. Colonies that grew on LB Apramycin plates but did not grow on LB hygromycin plates were selected.

The plasmid pFLP-hyg (contains genes necessary for flippase activity) was transformed into the pABSCR-negative *K. pneumoniae* with the correct inserts using the same electroporation settings as above. Successful transformants were selected was by plating on LB plates containing 100 ng/µl hygromycin, incubated at 30 °C overnight, streaked onto LB plates and heat shocked at 43 °C overnight. Individual colonies were selected and screened for successful removal of apramycin resistance cassette (markerless deletion) by simultaneously streaking on LB plates with and without 50 ng/µl apramycin. Colonies that were apramycin sensitive were screened for loss of pFLP-hyg plasmid by streaking on LB hygromycin plates and incubating at 30 °C overnight. Mutants were verified by PCR using confirmation sequencing primers as listed in Supplementary Table 3. The success of deletion of *lsrB* and *lsrD* genes was phenotypically confirmed by autoinducer-2 bioassay.

Verified mutants were tagged with mCherry via transformation with the pFA6a-mCherry plasmid carrying a hygromycin resistance marker. *K. pneumoniae* MGH78578 mutants were grown in 50 ml LB medium at 37 °C overnight and cells were collected by centrifugation (8000× *g*). Cells were washed by resuspending the cell pellet in 50 ml ice-cold sterile water and centrifugation (8000× *g*). Washing was repeated another three times and the final cell pellet was resuspended in 200 µl ice-cold H_2O. A 50 µl aliquot of electrocompetent cells were mixed with 100 ng of plasmid and transferred into an ice-cold electroporation cuvette (1 mm gap). Transformation (25 mF, 200 W, 5 ms pulse and 2 kV/cm) was carried out using a Gene Pulsar Electroporator (Biorad, Hercules, CA, USA). Two hundred fifty microliters of pre-warmed (37 °C) LB media (Thermo Fisher Scientific, MA, USA) was added to the transformed cells and this mixture was incubated with shaking for 1 h at 37 °C. Successful transformants were selected by plating on LB plates with 50 ng/µl hygromycin and incubated for 37 °C overnight and selecting for red-colored colonies the next day. The fluorescence of the tagged mutant strains were verified by confocal microscopy. The excitation and emission wavelengths used for confocal microscopy via mCherry was 587 and 610 nm, respectively.

Whole-genome sequencing of *K. pneumoniae* MGH78578 mutants

Genomic DNA was extracted using a Monarch DNA purification Kit (New England Biolabs, MA, USA) according to the instructions provided by the manufacturer. Purified genomic DNA libraries were generated using the Swift Biosciences Accel-NGS Plus DNA kit and sequenced using an Illumina HiSeq 2500. Genomic DNA sequencing reads were quality assessed and adapters were removed using the Trim Galore package (v0.6.4_dev). Low-quality ends were removed from sequences with a Phred score lower than 20. Paired reads were merged using PandaSeq (v2.11). The resulting reads were assembled using *K. pneumoniae* MGH78578 genome sequence

(accession number: CP000647) as a reference genome using Bowtie2 (v2.3.4.1.). SNP analyses was done using PARSNP (v1.5.2-1). Genomic DNA sequences of Δ*lsrB* and Δ*lsrD* mutants were compared to the wild-type for single-nucleotide polymorphisms (SNPs), insertions and deletions to validate correct deletion of genes and for the presence of secondary mutations.

Plasmid retention assay

Plasmid retention assay was performed to determine the rate of plasmid loss within *K. pneumoniae* strains. Plasmid retention assay was adapted as previously described[53]. Briefly, *K. pneumoniae* strains were grown overnight in M9CasGlucose (0.04% glucose) with appropriate antibiotic selection at room temperature. Cells were readjusted to OD_{600} = 0.5 and diluted 10^{-6} in M9CasGlucose without selective antibiotics and grown at room temperature at 100 rpm. Every 24 h, cultures were readjusted to OD_{600} = 0.5 and diluted 10^{-6} in M9CasGluose and grown at room temperature at 100 rpm. Every 24 h, starting from t = 0 h and ending at t = 72 h, serial dilutions of the cultures were plated on LB agar without antibiotic selection. Plasmid retention was measured by picking 100 colonies from the plate without selected antibiotics and growing them on plates with antibiotic selection. Plasmid loss was calculated by the proportion of colonies out of 100 that did not grow under antibiotic selection.

Autoinducer-2 bioassay

Autoinducer-2 (AI-2) bioassay was performed to determine the extracellular AI-2 concentration in the cell-free supernatant of *K. pneumoniae* mutant strains using an AI-2 reporter strain *Vibrio harveyi* BB170. AI-2 bioassay protocol was performed as previously described[17]. Briefly, test strains were inoculated in 5 ml M9CasGlucose medium (0.04% glucose) and incubated at room temperature with shaking overnight. A 5 µl aliquot of overnight cultures of *V. harveyi* BB170 (reporter strain) and *V. harveyi* BB152 (positive control strain) were diluted into 5 ml Autoinducer Bioassay (AB) medium (ATCC medium 2746) and incubated at 30 °C with shaking overnight. *V. harveyi* BB170 was diluted 1000× into fresh AB medium and 160 µl of this mixture was pipetted into 96-well plates. For AI-2 quantification in planktonic cultures, 40 µl aliquot of filter-sterilized (0.2-µm filter pore size) M9CasGlucose (negative control), overnight cultures of *V. Harveyi* BB152 grown in AB medium (positive control) and cell-free supernatants of test strains (grown overnight in AB medium at room temperature) were added into 160 µl of *V. harveyi* BB170 for a final volume of 200 µl per well in triplicates. For quantifying AI-2 from batch biofilms, 1 ml of supernatants from batch biofilms grown as above were collected at 12 and 24 h and filter-sterilized. For quantifying AI-2 from continuous-culture biofilms, 3 ml of flow-through from the flow cells containing biofilms were collected and filter-sterilized at 24, 48, and 72 h. The filter-sterilized supernatants from batch biofilms and the filter-sterilized flow-through from continuous-culture biofilms were added to *V. harveyi* BB170 grown in AB media as described above. Luminescence from 96-well plates was measured using a microplate reader (M200 Tecan) every 10 min for a total of 6 h. Relative Luminescence Units (RLU) was calculated (luminescence units of test strain/ luminescence units of negative control) and an ANOVA test was performed to determine significant differences in AI-2 concentration between mutant and wild-type *K. pneumoniae* MGH78578 strains. Three technical and three biological replicates were performed, and statistical analyses (one-way ANOVA test with correction for multiple testing via the Brown–Forsythe test) were carried out by GraphPad Prism (version 9 for windows, GraphPad software, La Jolla, California, USA, www.Graphpad.Com).

Generating complemented strains

Complementation was performed as previously described[15]. The full-length *lsrB* (1022 bp) and *lsrD* (1017 bp) genes were amplified from the *K. pneumoniae* MGH78578 wild-type using purified genomic DNA as the template (primers Supplementary Table S1). PCR was carried out with the following conditions: 98 °C initial denaturation step (30 s), 35 cycles of 98 °C denaturation (10 s), 55–70 °C annealing (30 s), and 72 °C extension (45 s) and a final extension step of 72 °C (120 s). The PCR product consisted of the full-length *lsrB* and *lsrD* genes flanked by *Eco*RI restriction site sequence at both ends. The *Eco*RI-flanked *lsrB* and *lsrD* genes as well as the pUCP22notI plasmid (Supplementary Table S1) were then digested with *Eco*RI (New England Biolabs, Ipswich, MA, USA) according to the manufacturer's instructions. The digested pUCPP22notI plasmid and *Eco*RI-flanked PCR products were ligated with T4 DNA ligase (Thermo Fisher, Waltham, MA, USA) according to the manufacturer's instructions to pUCPP22notI + *lsrB*/*lsrD* constructs. The ligated product was separated using gel electrophoresis and purified using gel elution. Successful ligation was verified using standard M13 primers (Supplementary Table S1). The verified pUCP22notI + *lsrB*/*lsrD* constructs were transformed into *K. pneumoniae* MGH78578 *lsrB*/*lsrD* mutants tagged with mCherry (Table 2) using the conditions listed above. Successful transformants were selected on LB plates with the addition of 100 ng/µl hygromycin and 50 ng/µl gentamicin. The success of complementation was verified by autoinducer-2 bioassay as described above.

Growth rate and biofilm experiments

K. pneumoniae MGH78578 strains were grown in M9 medium supplemented with casamino acids and glucose and were monitored by inoculating 96-well plates at an initial OD_{600} of 0.01 and incubating at room temperature for 16 h. OD_{600} readings were recorded every hour using a Tecan M200 microplate reader (Tecan Group Ltd., Männedorf, Switzerland) and analyzed using Graphpad prism. Growth rates were calculated for each strain using the formula: $[N_t = N_0 * (1+r)^t]$, where N_t: OD_{600} at time at the end of exponential growth rate, N_0: OD_{600} at time at the start of exponential growth rate, r: growth rate and t: time. Batch biofilm experiments were performed as described previously[54]. Overnight cultures were grown in M9 supplemented with casamino acids and glucose. Cultures were adjusted to an OD_{600} of 0.01 by diluting in the appropriate media and 1 ml of this suspension was distributed into a 24-well microtiter plate. After 24 h incubation at room temperature, the medium was removed and the wells were washed once with 1.5 ml sterile M9 medium to remove loosely attached cells. The biofilms were stained with 1.75 ml Crystal Violet (CV) solution (0.1% w/v). Unbound CV was removed by three washes with 2 ml of M9 medium. Finally, 2 ml of absolute ethanol was used to extract bound CV by incubating on a rotary shaker at 100 rpm for 10 min at RT. The OD_{580} (Tecan M200) was determined for 200 µl of the ethanol-CV extract. Statistical analyses were performed using Graphpad Prism (one-way or two-way ANOVA test with correction for multiple testing via the Brown–Forsythe or Dunnett's test, respectively).

Continuous flow-cell cultivation of biofilms and imaging with confocal microscopy

Monospecies and mixed-species biofilms were established in flow cells as previously described[15]. Biofilms were grown in triple-channel flow cells (1 × 4 × 40 mm per channel). Overnight cultures were grown in M9CasGlcuose and adjusted to 1×10^8 cells/ml by diluting in the same medium. For monospecies biofilms, 1×10^8 cells/ml was used as the inoculum. Mixed-species biofilms were prepared by mixing cultures of *P. aeruginosa* PAO1, *P. protegens* Pf-5 and *K. pneumoniae* MGH78578 in the ratio of 5:5:1. This was done by mixing 1×10^8 cells/ml cultures of volumes of 2.5 ml, 2.5 ml and 0.5 ml, respectively. Each channel was injected with 0.5 ml of inoculum mixture and the flow cell was inverted for 1 h to allow attachment of bacteria cells to flow cell surface. The flow cells were returned to an upright position and M9CasGlucose medium was then introduced via a peristaltic pump (flow rate of 9 ml/h) for 3 days to allow for biofilm maturation. After biofilms were established, they were imaged by confocal laser scanning microscopy (CLSM) (LSM780, Carl Zeiss, Singapore) at ×20 magnification using excitation and emission wavelengths for *P. aeruginosa* eYFP, *P. protegens* eCFP and *K. pneumoniae* mCherry of 514/527 nm, 458/476 nm, and 587/610 nm, respectively. For each of the three flow-cell channels, five Z-stack images were acquired starting from a spot on the center of the flow-cell channel, 5–10 mm from inlet. A total of 15 Z-stack

images were acquired for each flow cell, representing 15 technical replicates for each mixed-species biofilm combination. The experiments were independently repeated three times for each mixed-species biofilm combination. The image stacks were analyzed for biovolume and surface area using IMARIS (Bitplane AG, Belfast, UK). Statistical analyses were carried out by GraphPad Prism 9 (one-way or two-way ANOVA test with correction for multiple testing via the Brown–Forsythe or Dunnett's test, respectively).

Quantification of planktonic growth rate and batch biofilm biomass after addition of cell-free supernatants

To obtain cell-free supernatants (CFS), *K. pneumoniae* strains were grown in 5 ml M9CasGlcuose medium for 12 h. Cultures were centrifuged for 10 mins at 10,000 × *g* and supernatants were filtered with a syringe-filter (0.1 µm pore size). To obtain heat-treated and filtered CFS, CFS were heat-treated for 10 min at 65 °C and subjected to centrifugation using a Amicon Pro Purification System (Merck, NJ, USA) with a molecular weight cut-off of 3 Kda. This treatment of the CFS will result in the removal of most secreted proteins in the CFS and will only retain small molecules such as AI-2. Batch biofilms of *P. aeruginosa* and *P. protegens* were grown in 24-well plates as above. At the start of biofilm growth, 200 µl of either untreated CFS or heat-treated and filtered CFS were added to 800 µl of bacteria culture. After 24 h of biofilm growth at RT, biomass of biofilms was quantified by CV assay as described above. Planktonic growth rate was measured as above, with 20 µl CFS added to 180 µl of OD = 0.01 cultures of either *P. aeruginosa* or *P. protegens* at the start of the experiment.

Fitness assays in planktonic conditions

Planktonic competition assays between *K. pneumoniae* MGH78578 strains and *P. aeruginosa* PAO1/*P. protegens* Pf5 were carried out in M9CasGlucose medium. *K. pneumoniae* MGH78578 (wild-type and mutants) and *P. aeruginosa* PAO1/*P. protegens* Pf5 cultures grown overnight were diluted to 1×10^8 cells/ml. Equal volumes of *K. pneumoniae* MGH78578 mixtures were mixed with *P. aeruginosa* or *P. protegens* and incubated with shaking at RT. CFU counts of bacteria were determined at 0 and 24 h by dilution drop plating in triplicate on LB plates containing 100 µg/ml hygromycin and 30 µg/ml gentamicin. *K. pneumoniae* tagged with a plasmid carrying mCherry was selected on LB plates containing hygromycin, while *P. aeruginosa* and *P. protegens* containing gentamicin resistance gene were selected on LB plates containing gentamicin. Plates were incubated at room temperature and CFUs were counted the next day. To determine the proportions of each bacterial species, the following formula was used: *(Number of each bacterial species/total number of bacteria) x 100*. The fitness of each species in both the planktonic and surface-associated competition assay was calculated as: *Log [Fold change of mutant/fold change of wild-type]*. The difference in fitness and composition between wild-type and mutant groups was determined by ANOVA using GraphPad Prism 9 (two-way ANOVA test with correction for multiple testing via the Dunnett's test).

Autoaggregation assay

A settling assay was performed to determine the capability of the *K. pneumoniae* strains to autoaggregate rapidly and sediment to the bottom of the tube. The settling assay was performed as previously described[55]. *K. pneumoniae* strains were inoculated in 5 ml M9Cas medium supplemented with 0.04% glucose and grown overnight with shaking at RT. Overnight cultures were adjusted to approximately the same OD_{600} (0.2–0.4) with fresh medium and 15 ml of culture was transferred into a clear 20 ml glass tube. Before starting measurements, the cultures were vigorously shaken for 10 s. At the start of experiment ($t = 0$ min) and at 10 min intervals thereafter, three 100 µl samples were collected approximately 10 mm from the surface and transferred into wells of a 96-well microtiter plate and placed on ice. At the end of the experiment (final time point = 180 min), images of the tubes were collected and the OD_{600} of the samples in the 96-well microtiter plates were measured using a microplate reader (M200 Tecan). Three biological replicates were performed and statistical analyses were carried out by GraphPad Prism 9 (one-way ANOVA test with correction for multiple testing via the Brown–Forsythe test).

Reporting summary

Further information on research design is available in the Nature Research Reporting Summary linked to this article.

Data availability

All data generated or analyzed in this study are included in the published article.

Received: 14 February 2023; Accepted: 6 August 2024;
Published online: 28 September 2024

References

1. Hall-Stoodley, L., Costerton, J. W. & Stoodley, P. Bacterial biofilms: from the natural environment to infectious diseases. *Nat. Rev. Microbiol.* **2**, 95–108 (2004).
2. Camus, L., Briaud, P., Vandenesch, F. & Moreau, K. How bacterial adaptation to cystic fibrosis environment shapes interactions between *Pseudomonas aeruginosa* and *Staphylococcus aureus*. *Front. Microbiol.* **12**, 617784 (2021).
3. Okada, F. et al. Acute Klebsiella pneumoniae pneumonia alone and with concurrent infection: comparison of clinical and thin-section CT findings. *Br. J. Radiol.* **83**, 854–860 (2010).
4. Riedel, K. et al. N-acylhomoserine-lactone-mediated communication between *Pseudomonas aeruginosa* and *Burkholderia cepacia* in mixed biofilms. *Microbiology* **147**, 3249–3262 (2001).
5. Tytgat, H. L. P., Nobrega, F. L., van der Oost, J. & de Vos, W. M. Bowel biofilms: tipping points between a healthy and compromised gut? *Trends Microbiol.* **27**, 17–25 (2019).
6. Elias, S. & Banin, E. Multi-species biofilms: living with friendly neighbors. *FEMS Microbiol. Rev.* **36**, 990–1004 (2012).
7. Nielsen, A. T., Tolker-Nielsen, T., Barken, K. B. & Molin, S. Role of commensal relationships on the spatial structure of a surface-attached microbial consortium. *Environ. Microbiol.* **2**, 59–68 (2000).
8. Yoshida, S., Ogawa, N., Fujii, T. & Tsushima, S. Enhanced biofilm formation and 3-chlorobenzoate degrading activity by the bacterial consortium of Burkholderia sp. NK8 and *Pseudomonas aeruginosa* PAO1. *J. Appl. Microbiol.* **106**, 790–800 (2009).
9. Jackson, G., Beyenal, H., Rees, W. M. & Lewandowski, Z. Growing reproducible biofilms with respect to structure and viable cell counts. *J. Microbiol. Methods* **47**, 1–10 (2001).
10. Stoodley, P. et al. Growth and detachment of cell clusters from mature mixed-species biofilms. *Appl. Environ. Microbiol.* **67**, 5608–5613 (2001).
11. Lee, K. W. K. et al. Biofilm development and enhanced stress resistance of a model, mixed-species community biofilm. *ISME J.* **8**, 894–907 (2014).
12. Chazal, P. M. Pollution of modern metalworking fluids containing biocides by pathogenic bacteria in France. Reexamination of chemical treatments accuracy. *Eur. J. Epidemiol.* **11**, 1–7 (1995).
13. Anand, A. A. P. et al. Isolation and characterization of bacteria from the gut of Bombyx mori that degrade cellulose, xylan, pectin and starch and their impact on digestion. *J. Insect Sci.* **10**, 107–107 (2010).
14. Periasamy, S. et al. Pseudomonas aeruginosa PAO1 exopolysaccharides are important for mixed species biofilm community development and stress tolerance. *Front. Microbiol.* **6**, 851 (2015).
15. Subramoni, S., Muzaki, M., Booth, S. C. M., Kjelleberg, S. & Rice, S. A. N-Acyl homoserine lactone-mediated quorum sensing regulates species interactions in multispecies biofilm communities. *Front Cell Infect. Microbiol.* **11**, 646991 (2021).
16. Schauder, S., Shokat, K., Surette, M. G. & Bassler, B. L. The LuxS family of bacterial autoinducers: biosynthesis of a novel quorum-sensing signal molecule. *Mol. Microbiol.* **41**, 463–476 (2001).

17. Surette, M. G. & Bassler, B. L. Quorum sensing in *Escherichia coli* and *Salmonella typhimurium*. *Proc. Natl. Acad. Sci. USA* **95**, 7046–7050 (1998).
18. Bassler, B. L., Wright, M., Showalter, R. E. & Silverman, M. R. Intercellular signalling in *Vibrio harveyi*: sequence and function of genes regulating expression of luminescence. *Mol. Microbiol.* **9**, 773–786 (1993).
19. Vidal, J. E., Ludewick, H. P., Kunkel, R. M., Zähner, D. & Klugman, K. P. The LuxS-dependent quorum-sensing system regulates early biofilm formation by *Streptococcus pneumoniae* strain D39. *Infect. Immun.* **79**, 4050–4060 (2011).
20. Zhao, L., Xue, T., Shang, F., Sun, H. & Sun, B. *Staphylococcus aureus* AI-2 quorum sensing associates with the KdpDE two-component system to regulate capsular polysaccharide synthesis and virulence. *Infect. Immun.* **78**, 3506–3515 (2010).
21. González Barrios, A. F. et al. Autoinducer 2 controls biofilm formation in *Escherichia coli* through a novel motility quorum-sensing regulator (MqsR, B3022). *J. Bacteriol.* **188**, 305–316 (2006).
22. Zhu, H., Liu, H. J., Ning, S. J. & Gao, Y. L. A luxS-dependent transcript profile of cell-to-cell communication in Klebsiella pneumoniae. *Mol. Biosyst.* **7**, 3164–3168 (2011).
23. Zhu, H., Liu, H. J., Ning, S. J. & Gao, Y. L. The response of type 2 quorum sensing in *Klebsiella pneumoniae* to a fluctuating culture environment. *DNA Cell Biol.* **31**, 455–459 (2012).
24. Wang, S., Payne, G. F. & Bentley, W. E. Quorum sensing communication: molecularly connecting cells, their neighbors, and even devices. *Annu. Rev. Chem. Biomol. Eng.* **11**, 447–468 (2020).
25. Laganenka, L., Colin, R. & Sourjik, V. Chemotaxis towards autoinducer 2 mediates autoaggregation in *Escherichia coli*. *Nat. Commun.* **7**, 12984 (2016).
26. Xavier, K. B. & Bassler, B. L. Regulation of uptake and processing of the quorum-sensing autoinducer AI-2 in *Escherichia coli*. *J. Bacteriol.* **187**, 238–248 (2005).
27. McNab, R. et al. LuxS-based signaling in *Streptococcus gordonii*: autoinducer 2 controls carbohydrate metabolism and biofilm formation with *Porphyromonas gingivalis*. *J. Bacteriol.* **185**, 274–284 (2003).
28. Balestrino, D., Haagensen, J. A., Rich, C. & Forestier, C. Characterization of type 2 quorum sensing in *Klebsiella pneumoniae* and relationship with biofilm formation. *J. Bacteriol.* **187**, 2870–2880 (2005).
29. Chen, L. et al. Investigation of LuxS-mediated quorum sensing in *Klebsiella pneumoniae*. *J. Med. Microbiol.* **69**, 402–413 (2020).
30. Li, H. et al. Autoinducer-2 facilitates *Pseudomonas aeruginosa* PAO1 pathogenicity in vitro and in vivo. *Front. Microbiol.* **8**, 1944 (2017).
31. Li, H. et al. Autoinducer-2 regulates *Pseudomonas aeruginosa* PAO1 biofilm formation and virulence production in a dose-dependent manner. *BMC Microbiol.* **15**, 192 (2015).
32. Taga, M. E., Miller, S. T. & Bassler, B. L. Lsr-mediated transport and processing of AI-2 in *Salmonella typhimurium*. *Mol. Microbiol.* **50**, 1411–1427 (2003).
33. Pereira, C. S., de Regt, A. K., Brito, P. H., Miller, S. T. & Xavier, K. B. Identification of functional LsrB-like autoinducer-2 receptors. *J. Bacteriol.* **191**, 6975–6987 (2009).
34. Xavier, K. B. & Bassler, B. L. LuxS quorum sensing: more than just a numbers game. *Curr. Opin. Microbiol.* **6**, 191–197 (2003).
35. Zhang, Y. et al. LsrB-based and temperature-dependent identification of bacterial AI-2 receptor. *AMB Express* **7**, 188 (2017).
36. Hajishengallis, G. et al. Low-abundance biofilm species orchestrates inflammatory periodontal disease through the commensal microbiota and complement. *Cell Host Microbe* **10**, 497–506 (2011).
37. Hansen, S. K., Rainey, P. B., Haagensen, J. A. & Molin, S. Evolution of species interactions in a biofilm community. *Nature* **445**, 533–536 (2007).
38. Hibbing, M. E., Fuqua, C., Parsek, M. R. & Peterson, S. B. Bacterial competition: surviving and thriving in the microbial jungle. *Nat. Rev. Microbiol.* **8**, 15–25 (2010).
39. Zuo, J. et al. Lsr operon is associated with AI-2 transfer and pathogenicity in avian pathogenic *Escherichia coli*. *Vet. Res.* **50**, 109 (2019).
40. Armbruster, C. E. et al. RbsB (NTHI_0632) mediates quorum signal uptake in nontypeable *Haemophilus influenzae* strain 86-028NP. *Mol. Microbiol.* **82**, 836–850 (2011).
41. Shao, H., James, D., Lamont, R. J. & Demuth, D. R. Differential interaction of *Aggregatibacter* (*Actinobacillus*) *actinomycetemcomitans* LsrB and RbsB proteins with autoinducer 2. *J. Bacteriol.* **189**, 5559–5565 (2007).
42. Pereira, C. S., Thompson, J. A. & Xavier, K. B. AI-2-mediated signalling in bacteria. *FEMS Microbiol. Rev.* **37**, 156–181 (2013).
43. De Araujo, C., Balestrino, D., Roth, L., Charbonnel, N. & Forestier, C. Quorum sensing affects biofilm formation through lipopolysaccharide synthesis in *Klebsiella pneumoniae*. *Res. Microbiol.* **161**, 595–603 (2010).
44. Brenner, K. & Arnold, F. H. Self-organization, layered structure, and aggregation enhance persistence of a synthetic biofilm consortium. *PLoS ONE* **6**, e16791 (2011).
45. Liu, W. et al. Interspecific bacterial interactions are reflected in multispecies biofilm spatial organization. *Front. Microbiol.* **7**, 1366 (2016).
46. Zhang, L. et al. Sensing of autoinducer-2 by functionally distinct receptors in prokaryotes. *Nat. Commun.* **11**, 5371 (2020).
47. Basler, M., Ho, B. T. & Mekalanos, J. J. Tit-for-tat: type VI secretion system counterattack during bacterial cell-cell interactions. *Cell* **152**, 884–894 (2013).
48. Li, E., Wu, J. & Zhang, D. Exogenous autoinducer-2 inhibits biofilm development of Desulfovibrio sp. Huiquan2017. *World J. Microbiol. Biotechnol.* **37**, 124 (2021).
49. Jang, Y. J., Choi, Y. J., Lee, S. H., Jun, H. K. & Choi, B. K. Autoinducer 2 of *Fusobacterium nucleatum* as a target molecule to inhibit biofilm formation of periodontopathogens. *Arch. Oral. Biol.* **58**, 17–27 (2013).
50. Jang, Y. J., Sim, J., Jun, H. K. & Choi, B. K. Differential effect of autoinducer 2 of *Fusobacterium nucleatum* on oral streptococci. *Arch. Oral. Biol.* **58**, 1594–1602 (2013).
51. Stewart, P. S., Camper, A. K., Handran, S. D., Huang, C. & Warnecke, M. Spatial distribution and coexistence of *Klebsiella pneumoniae* and *Pseudomonas aeruginosa* in biofilms. *Micro. Ecol.* **33**, 2–10 (1997).
52. Huang, T. W. et al. Capsule deletion via a λ-Red knockout system perturbs biofilm formation and fimbriae expression in *Klebsiella pneumoniae* MGH 78578. *BMC Res. Notes* **7**, 13 (2014).
53. Chen, J., Yoong, P., Ram, G., Torres, V. J. & Novick, R. P. Single-copy vectors for integration at the SaPI1 attachment site for *Staphylococcus aureus*. *Plasmid* **76**, 1–7 (2014).
54. Schleheck, D. et al. Pseudomonas aeruginosa PAO1 preferentially grows as aggregates in liquid batch cultures and disperses upon starvation. *PLoS ONE* **4**, e5513 (2009).
55. Hasman, H., Chakraborty, T. & Klemm, P. Antigen-43-mediated autoaggregation of *Escherichia coli* is blocked by fimbriation. *J. Bacteriol.* **181**, 4834–4841 (1999).
56. Wang, N. et al. The novel proteins Rng8 and Rng9 regulate the myosin-V Myo51 during fission yeast cytokinesis. *J. Cell Biol.* **205**, 357–375 (2014).
57. Olsen, R. H., DeBusscher, G. & McCombie, W. R. Development of broad-host-range vectors and gene banks: self-cloning of the Pseudomonas aeruginosa PAO chromosome. *J. Bacteriol.* **150**, 60–69 (1982).

Acknowledgements

The authors would like to acknowledge the financial support from the National Research Foundation and the Ministry of Education Singapore under its Research Centre of Excellence Program. The research was also

supported by a grant from the Singapore Ministry of Education (MOE2019-T2-1-050) and the Australian Research Council project DP230101760.

Author contributions

M.Z.B.M.M., Subramoni, and Summers undertook the experimental work. M.Z.B.M.M., Subramoni, Summers, S.A.R., and S.K. contributed to data analysis and interpretation. M.Z.B.M.M., S.A.R., and S.K. designed the project as well as preparation of the manuscript.

Competing interests

The authors declare no competing interests.

Additional information

Supplementary information The online version contains supplementary material available at https://doi.org/10.1038/s41522-024-00546-0.

Correspondence and requests for materials should be addressed to Muhammad Zulfadhly Bin Mohammad Muzaki or Scott A. Rice.